U.S. DEPARTMENT OF COMMERCE
National Technical Information Service

PB-251 580

Effects of Gaseous Pollutants on Materials: A Chamber Study

Environmental Sciences Research Lab.

February 1976

KEEP UP TO DATE

Between the time you ordered this report—which is only one of the hundreds of thousands in the NTIS information collection available to you—and the time you are reading this message, several *new* reports relevant to your interests probably have entered the collection.

Subscribe to the **Weekly Government Abstracts** series that will bring you summaries of new reports *as soon as they are received by NTIS* from the originators of the research. The WGA's are an NTIS weekly newsletter service covering the most recent research findings in 25 areas of industrial, technological, and sociological interest—invaluable information for executives and professionals who must keep up to date.

The executive and professional information service provided by NTIS in the **Weekly Government Abstracts** newsletters will give you thorough and comprehensive coverage of government-conducted or sponsored research activities. And you'll get this important information within two weeks of the time it's released by originating agencies.

WGA newsletters are computer produced and electronically photocomposed to slash the time gap between the release of a report and its availability. You can learn about technical innovations immediately—and use them in the most meaningful and productive ways possible for your organization. Please request NTIS-PR-205/PCW for more information.

The weekly newsletter series will keep you current. But *learn what you have missed in the past* by ordering a computer **NTISearch** of all the research reports in your area of interest, dating as far back as 1964, if you wish. Please request NTIS-PR-186/PCN for more information.

WRITE: Managing Editor
5285 Port Royal Road
Springfield, VA 22161

Keep Up To Date With SRIM

SRIM (Selected Research in Microfiche) provides you with regular, automatic distribution of the complete texts of NTIS research reports *only* in the subject areas you select. SRIM covers almost all Government research reports by subject area and/or the originating Federal or local government agency. You may subscribe by any category or subcategory of our WGA **(Weekly Government Abstracts)** or **Government Reports Announcements and Index** categories, or to the reports issued by a particular agency such as the Department of Defense, Federal Energy Administration, or Environmental Protection Agency. Other options that will give you greater selectivity are available on request.

The cost of SRIM service is only 45¢ domestic (60¢ foreign) for each complete microfiched report. Your SRIM service begins as soon as your order is received and processed and you will receive biweekly shipments thereafter. If you wish, your service will be backdated to furnish you microfiche of reports issued earlier.

Because of contractual arrangements with several Special Technology Groups, not all NTIS reports are distributed in the SRIM program. You will receive a notice in your microfiche shipments identifying the exceptionally priced reports not available through SRIM.

A deposit account with NTIS is required before this service can be initiated. If you have specific questions concerning this service, please call (703) 451-1558, or write NTIS, attention SRIM Product Manager.

This information product distributed by

NTIS U.S. DEPARTMENT OF COMMERCE
National Technical Information Service
5285 Port Royal Road
Springfield, Virginia 22161

092119

PB 251 580

EPA-600/3-76-015
February 1976

Ecological Research Series

REPRODUCED BY
NATIONAL TECHNICAL
INFORMATION SERVICE
U. S. DEPARTMENT OF COMMERCE
SPRINGFIELD, VA. 22161

RESEARCH REPORTING SERIES

Research reports of the Office of Research and Development, U.S. Environmental Protection Agency, have been grouped into five series. These five broad categories were established to facilitate further development and application of environmental technology. Elimination of traditional grouping was consciously planned to foster technology transfer and a maximum interface in related fields. The five series are:

1. Environmental Health Effects Research
2. Environmental Protection Technology
3. Ecological Research
4. Environmental Monitoring
5. Socioeconomic Environmental Studies

This report has been assigned to the ECOLOGICAL RESEARCH series. This series describes research on the effects of pollution on humans, plant and animal species, and materials. Problems are assessed for their long- and short-term influences. Investigations include formation, transport, and pathway studies to determine the fate of pollutants and their effects. This work provides the technical basis for setting standards to minimize undesirable changes in living organisms in the aquatic, terrestrial, and atmospheric environments.

This document is available to the public through the National Technical Information Service, Springfield, Virginia 22161.

TECHNICAL REPORT DATA
(Please read Instructions on the reverse before completing)

1. REPORT NO.	2.	3. RECIPIENT'S ACCESSION NO.
EPA-600/3-76-015		

4. TITLE AND SUBTITLE	5. REPORT DATE
EFFECTS OF GASEOUS POLLUTANTS ON MATERIALS-- A CHAMBER STUDY	February 1976
	6. PERFORMING ORGANIZATION CODE
7. AUTHOR(S)	8. PERFORMING ORGANIZATION REPORT NO.
F. H. Haynie, J. W. Spence and J. B. Upham	
9. PERFORMING ORGANIZATION NAME AND ADDRESS	10. PROGRAM ELEMENT NO.
Environmental Sciences Research Laboratory Office of Research and Development U.S. Environmental Protection Agency Research Triangle Park, N.C. 27711	1AA008
	11. CONTRACT/GRANT NO.
12. SPONSORING AGENCY NAME AND ADDRESS	13. TYPE OF REPORT AND PERIOD COVERED
same as block 9	Inhouse
	14. SPONSORING AGENCY CODE EPA-ORD

15. SUPPLEMENTARY NOTES

16. ABSTRACT

This document describes a comprehensive laboratory study using specially designed controlled environment exposure chambers to assess the effects of gaseous air pollutants (sulfur dioxide, nitrogen dioxide, and ozone) on a variety of materials. Materials included weathering steel, galvanized steel, aluminum alloy, paints, drapery fabrics, white sidewall tire rubber, vinyl house siding, and marble. The exposure experiment was statistically designed using a two-level factorial arrangement to identify the environmental factors or combination of factors, or both, that cause materials damage. Over 200 different direct and synergistic effects were examined. The study revealed that only 22 of the possible effects were statistically significant at better than a 95 percent confidence level. Sulfur dioxide, relative humidity, and the interaction between them, were the main factors causing effects. A number of empirical functions were developed that relate materials effects to various factors causing the effects. An exceptionally good relationship was obtained for the corrosion of weathering steel.

The lack of statistical significance that was found for the large majority of effects that were studied is equally as important as the significant effects. As a result a large number of material-pollutant combinations may be excluded from further detailed study.

17. KEY WORDS AND DOCUMENT ANALYSIS

a. DESCRIPTORS	b. IDENTIFIERS/OPEN ENDED TERMS	c. COSATI Field/Group
Experimental design Statistical analysis *Test chambers Air Pollution *Sulfur dioxide *Nitrogen dioxide *Ozone *Degradation *Materials		14B 13B 07B 14G 11 12A

PRICES SUBJECT TO CHANGE

18. DISTRIBUTION STATEMENT	19. SECURITY CLASS (This Report)	21. NO. OF PAGES
RELEASE TO PUBLIC	UNCLASSIFIED	98
	20. SECURITY CLASS (This page)	22. PRICE
	UNCLASSIFIED	$5.00

EPA Form 2220-1 (9-73)

EFFECTS OF GASEOUS POLLUTANTS ON MATERIALS--A CHAMBER STUDY

by

F. H. Haynie
J. W. Spence
J. B. Upham

Environmental Sciences Research Laboratory
Research Triangle Park, North Carolina, 27711

U.S. ENVIRONMENTAL PROTECTION AGENCY
OFFICE OF RESEARCH AND DEVELOPMENT
ENVIRONMENTAL SCIENCES RESEARCH LABORATORY
RESEARCH TRIANGLE PARK, NORTH CAROLINA, 27711

DISCLAIMER

This report has been reviewed by the Environmental Sciences Research Laboratory, U.S. Environmental Protection Agency, and approved for publication. Mention of trade names or commercial products does not constitute endorsement or recommendation for use.

ABSTRACT

This document describes a comprehensive laboratory study using specially designed controlled environment exposure chambers to assess the effects of gaseous air pollutants (sulfur dioxide, nitrogen dioxide, and ozone) on a variety of materials. Materials included weathering steel, galvanized steel, aluminum alloy, paints, drapery fabrics, white sidewall tire rubber, vinyl house siding, and marble. The exposure experiment was statistically designed using a two-level factorial arrangement to identify the environmental factors or combination of factors, or both, that cause materials damage. Over 200 different direct and synergistic effects were examined. The study revealed that only 22 of the possible effects were statistically significant at better than a 95 percent confidence level. Sulfur dioxide, relative humidity, and the interaction between them, were the main factors causing effects. A number of empirical functions were developed that relate materials effects to various factors causing the effects. An exceptionally good relationship was obtained for the corrosion of weathering steel.

The lack of statistical significance that was found for the large majority of effects that were studied is equally as important as the significant effects. As a result a large number of material-pollutant combinations may be excluded from further detailed study.

CONTENTS

		Page
	ABSTRACT	iii
	LIST OF FIGURES	vii
	LIST OF TABLES	ix
I	INTRODUCTION	1
II	SUMMARY	2
III	CONCLUSIONS	4
IV	RECOMMENDATIONS	5
V	EXPOSURE SYSTEM Design Features Evaluation of the System Chamber Lighting Chamber Pollutant Distribution Control Capability of Environmental Factors	6
VI	STUDY DESIGN Selection of Materials Statistical Design of Exposure Experiment Treatment of Data	12
VII	MATERIALS TESTING TECHNIQUES AND EVALUATION Testing Techniques Evaluation	17
VIII	EFFECTS ON WEATHERING STEEL Methodology Results and Discussion	21
IX	EFFECTS ON GALVANIZED STEEL Methodology Results and Discussion	32
X	EFFECTS ON ALUMINUM ALLOY Methodology Results and Discussion	38

Preceding page blank

CONTENTS

		Page
XI	EFFECTS ON PAINTS	47
	Methodology	
	Results and Discussion	
XII	EFFECTS ON DYED FABRICS	59
	Methodology	
	Results and Discussion	
XIII	EFFECTS ON ELASTOMERS AND PLASTICS	71
	Methodology	
	Results and Discussion	
XIV	EFFECTS ON MARBLE AND CEMENT	79
	Methodology	
	Results and Discussion	
XV	REFERENCES	84

LIST OF FIGURES

Figure		Page
1.	Exposure System Flow Diagram	7
2.	Temperature-Time Profiles for Exposed Metal Panels during Chamber Dew/Light Cycles	25
3.	Comparison of Predicted and Measured Thickness-Loss Values for Weathering Steel Exposed to Laboratory Controlled Polluted Air and Clean Air Conditions	29
4.	Comparison of Predicted and Actual Thickness-Loss Values for Galvanized Steel Exposed to Laboratory Controlled Polluted Air and Clean Air Conditions	35
5.	Scanning Electron Photomicrograph of an Exposed Galvanized Steel Panel Showing Uniformly Dispersed Crystalline Material Over the Zinc Surface	37
6.	Method of Stressing C-Ring Specimens	39
7.	Wiring of Specimens to Record Times-of-Failure	40
8.	Stress Induced Intergranular Cracks in Aluminum Alloy 7075-T35 after 1000 Hours Exposure to Air Containing SO_2	41
9.	Fracture Face Cross Section of Aluminum Alloy Specimen Ruptured by Bending after Intergranular Cracks Developed During 1000 Hours Exposure to Air Containing SO_2	42
10.	Stress Corrosion Crack after 2000 Hours Exposure to Clean Air	46
11.	Comparison of Predicted and Measured Fading Values for the Plum Colored Fabric Exposed to Laboratory Controlled Polluted Air and Clean Air Conditions	68
12.	Effect of Nitrogen Dioxide Concentration on the Fading of the Plum Colored Fabric	70
13.	Macrographs of Cracks Developed by White Sidewall Rubber Tire Specimens when Exposed Under High Stress to Designated Controlled Polluted Air Environmental Conditions for 1000 Hours	74

LIST OF FIGURES

Figure		Page
14.	SEM Photomicrograph (500K) of Marble Specimen Exposed for 1000 Hours to High Levels of Pollutants and High Relative Humidity	81
15.	Sulfur X-Ray Microprobe Scan (500K) of Marble Specimen Shown in Figure 14	81

LIST OF TABLES

Table		Page
1.	Statistically Significant Factors that Damaged Materials Exposed to Controlled Polluted Air Environmental Conditions	3
2.	Analysis of Variance of Xenon Lamp Energy Data	8
3.	Analysis of Variance of Pollutant (NO_2) Distribution within the Chambers	9
4.	Control Capability of Environmental Factors within the Chambers	10
5.	Ranking of Materials According to Estimated Damage by Gaseous Pollutants	12
6.	Materials Selected for the Chamber Exposure Study	13
7.	Environmental Factors and Levels Used in the Chamber Exposure Experiment	14
8.	Two-Level Factorial Arrangement	15
9.	Materials Testing Techniques	17
10.	Rate of Loss of Film Thickness During the Dew/Light Cycle Exposure Condition	18
11.	Rate of Loss of Film Thickness During the Constant Temperature and Humidity Exposure Condition	18
12.	Analysis of Variance for Rayon Tire Cord Breaking Strength	19
13.	Elemental Analysis of Weathering Steel	21
14.	Corrosion Rates of Weathering Steel Exposed to Designated Controlled Polluted Air Environmental Conditions	22
15.	Corrosion Rates of Weathering Steel Exposed to Designated Controlled Clean Air Environmental Conditions	23
16.	Analysis of Variance of Weathering Steel Corrosion Data for Polluted Air Exposure Conditions	24
17.	Analysis of Variance of Weathering Steel Corrosion Data for Clean Air Exposure Conditions	24

LIST OF TABLES

Table		Page
18.	Time-of-Panel-Wetness per Dew/Light Cycle and Geometric Mean Panel Temperature when Wet as a Function of Input Temperature and Relative Humidity	26
19.	Factors Affecting Atmospheric Corrosion of Weathering Steel Exposed at Urban Sites	30
20.	Corrosion Predictability as Measured by Coefficients of Variation, R^2, between Predicted and Field Values	31
21.	Corrosion Rates of Galvanized Steel Exposed to Designated Controlled Polluted Air Environmental Conditions	33
22.	Analysis of Variance of Galvanized Steel Corrosion Data for Polluted Air Exposure Conditions	33
23.	Elemental Analysis of Aluminum Alloy 7005-T53	38
24.	Bending Strength of Aluminum Alloy Stress Corrosion Specimens after Exposure to Designated Controlled Polluted Air Environmental Conditions for 1000 Hours	43
25.	Bending Strength of Aluminum Alloy Stress Corrosion Specimens after Exposure to Designated Controlled Clean Air Environmental Conditions for 1000 Hours	44
26.	Nominal Paint Film Thickness on Exposed Panels	47
27.	Factors for Converting Loss-in-Weight to Loss-in-Film-Thickness	49
28.	Erosion Rates of Oil Base House Paint Exposed to Designated Controlled Polluted Air Environmental Conditions	50
29.	Erosion Rates of Oil Base House Paint Exposed to Designated Controlled Clean Air Environmental Conditions	50
30.	Analysis of Variance of Oil Base House Paint Erosion Rates for Polluted Air Exposure Conditions	51
31.	Erosion Rates of Vinyl Coil Coating Exposed to Designated Controlled Polluted Air Environmental Conditions	54

LIST OF TABLES

Table		Page
32.	Erosion Rates of Vinyl Coil Coating Exposed to Designated Controlled Clean Air Environmental Conditions	54
33.	Analysis of Variance of Vinyl Coil Coating Erosion Rates for Polluted Air Exposure Conditions	55
34.	Erosion Rates of Acrylic Coil Coating Exposed to Designated Controlled Polluted Air Environmental Conditions	56
35.	Erosion Rates of Acrylic Coil Coating Exposed to Designated Controlled Clean Air Environmental Conditions	57
36.	Analysis of Variance of Acrylic Coil Coating Erosion Rates for Polluted Exposure Conditions	58
37.	Description of Drapery Fabrics	59
38.	Initial Fading Rates of Drapery Fabrics Exposed to Designated Controlled Polluted Air Environmental Conditions	61
39.	Initial Fading Rates of Drapery Fabrics Exposed to Designated Controlled Clean Air Environmental Conditions	62
40.	Analysis of Variance of Royal Blue Fabric Fading Rates for Polluted Air Exposure Conditions	63
41.	Analysis of Variance of Red Fabric Fading Rates for Polluted Air Exposure Conditions	64
42.	Analysis of Variance of Plum Fabric Fading Rates for Polluted Air Exposure Conditions	65
43.	Analysis of Variance of Fading Rates for Clean Air Exposure Conditions	66
44.	Cord Breaking Strength of White Sidewall Rubber Tire Specimens Exposed under Stress to Designated Controlled Polluted Air Environmental Conditions for 1000 Hours	73
45.	Analysis of Variance of Tire Cord Breaking Strength for Statistically Significant Factors	74

LIST OF TABLES

Table		Page
46.	Cracking Rates of White Sidewall Rubber Tire Specimens Exposure under Stress to Designated Controlled Polluted Air Environmental Conditions	76
47.	Analysis of Variance of Rubber Cracking Rates for Statistically Significant Factors	76
48.	Erosion Rates of Marble Exposed to Designated Controlled Polluted Air Environmental Conditions	82
49.	Analysis of Variance of Marble Erosion Rates for Polluted Air Exposure Conditions	82

SECTION I

INTRODUCTION

The Clean Air Amendments of 1970[1] call for research on the effects of air pollutants on materials. Such information is needed to serve as input for cost-benefit studies and as criteria for developing secondary air quality standards. As the first step in meeting this mandate, EPA investigators conducted surveys of the literature and of industrial organizations to identify and assess known effects of air pollutants on various materials. The result was a compilation of a number of documented materials-effects problems. The type of information documented, however, was too general and lacked such necessary details as dose-response relationships. Comprehensive laboratory research and supporting field studies were therefore deemed necessary.

This report describes the results of an initial laboratory study to statistically identify the direct and synergistic effects of gaseous pollutants (sulfur dioxide, ozone, and nitrogen dioxide), temperature, and humidity on several classes of materials. The laboratory study was conducted in specially designed controlled environment exposure chambers. Further laboratory and field exposure studies, based on the results of this initial study were to be conducted in order to develop damage predictive equations from dose-response data. These plans, as well as all materials research, however, have been terminated because of budgetary limitations and low priority.

SECTION II

SUMMARY

Fourteen different economically important materials were exposed to 16 different combinations of SO_2, O_3, NO_2, and relative humidity levels in laboratory controlled environment chambers. The environmental factors and twelve of the materials are presented as a matrix in Table 1. Specimens of latex house paint and cement were also exposed but the damage assessment technique produced unuseable data. The aluminum alloy and white sidewall tire rubber were exposed at two different stress levels to study the direct and synergistic effects of that factor on those two materials.

The statistically designed two-level factorial experiment made it possible to study 242 different direct and synergistic environmental effects. Poor data for the latex house paint and the cement reduced the number of possible effects to 212. The study revealed that only 22 of the possible effects were statistically significant at better than a 95 percent probability level. These effects are indicated in Table 1.

It is equally important to note the effects that were not statistically significant, because these represent possible areas of study that no longer need to be considered. For example, no significant effects were observed on the acrylic coil coating and the vinyl siding, and only relative humidity affected the blue and red fabrics. Thus, negative results would be expected from any further studies of these materials and pollutants.

When the magnitude of damage and the economics of material selection and replacement are considered, the vinyl coil coatings, the plum fabric, and the white sidewall tire rubber are not appreciably affected by these pollutants. The remaining materials are affected mainly by SO_2, relative humidity, and the interaction between these two factors.

Table 1. STATISTICALLY SIGNIFICANT FACTORS THAT DAMAGED MATERIALS EXPOSED TO CONTROLLED POLLUTED AIR ENVIRONMENTAL CONDITIONS

Factor \ Material	Weathering steel	Galvanized steel	Aluminum alloy	Oil base house paint	Vinyl coil coating	Acrylic coil coating	Blue fabric	Red fabric	Plum fabric	White sidewall tire rubber	Vinyl house siding	Marble
SO_2	■	■	■	■	◢							■
RH	■	■					■	■	■	◢		◢
O_3										■		◢
NO_2									■			
SO_2 x RH	◢											
SO_2 x O_3												
SO_2 x NO_2												
RH x O_3					◢					◢		
RH x NO_2					◢				◢			
O_3 x NO_2										■		
SO_2 x RH x O_3												
SO_2 x RH x NO_2												
SO_2 x O_3 x NO_2												
RH x O_3 x NO_2												
SO_2 x RH x O_3 x NO_2												

■, ◢ Significant at the 99 and 95 percent probability levels, respectively.
RH, Relative humidity
x means interacting with

NOTE: Both the aluminum stress corrosion specimens and the rubber were stressed at two different levels, thus the effects of stress and the interactions of stress with the 15 above factors were also possible, adding 32 additional possible effects.

SECTION III

CONCLUSIONS

Based on the results of a statistically designed controlled environment chamber study it is concluded that:

1. Sulfur dioxide at ambient levels contributes significantly to the corrosion of weathering steel and galvanized steel.

2. Sulfur dioxide at ambient levels contributes significantly to the erosion of oil base house paints containing calcium carbonates and marble.

3. Sulfur dioxide at ambient levels contributes significantly to the stress-corrosion cracking of 7005 T-6 aluminum alloy.

4. Vinyl and acrylic coil coatings, two drapery fabrics, white sidewall tire rubber and vinyl house siding were not significantly affected, either statistically or economically, by SO_2, NO_2, or O_3 at ambient levels.

5. The damage assessment techniques used for the latex house paint and the cement produced data too poor to analyze.

SECTION IV

RECOMMENDATIONS

Both laboratory and field studies should be initiated to determine dose-response relationships for the effects of sulfur dioxide on the following materials:

1. Weathering steel
2. Galvanized steel
3. Oil base house paint
4. Latex house paint
5. 7000 series aluminum alloy under stress
6. Marble
7. Cement

The laboratory study should be statistically designed to include five levels each for SO_2, temperature, relative humidity, and time. The SO_2 levels should range around existing annual average ambient air quality standards.

Field studies should be long enough to show non linear accumulative effects of SO_2.

SECTION V

EXPOSURE SYSTEM

DESIGN FEATURES

Controlled environment chambers provide the best means for generating materials effects data. For this study a sophisticated exposure system consisting of five chambers was designed and built.[2] The chambers operated at temperatures, relative humidities, and pollutant levels normally found to exist in ambient environments. To accelerate the environmental effects, however, a programmed dew/light cycle became a unique feature of each chamber. The dew/light cycle simulated day/night conditions, but could be repeated many times during a 24-hour period.

Figure 1 shows the basic flow diagram of the exposure system. Ambient air, after being filtered to remove particulate (>5μ) and gaseous pollutants, was cooled and dehumidified. The conditioned, clean air then flowed into five separate ducts (one for each chamber), each containing heater and steam humidification units, which reconditioned the air to a desired temperature and relative humidity. From each duct the air entered a mixing box that housed temperature and humidity control sensors and three gaseous pollutant (SO_2, NO_2, O_3) injection ports. The reconditioned, polluted air next flowed into the base of the chambers, across a plenum to facilitate mixing, up over the test specimens, out of the chambers into a decontamination unit, and finally to the outside.

To provide for a dew/light cycle, each exposure chamber featured a xenon arc lamp (6000 W) to simulate sunlight and chill racks upon which material test specimens were mounted. With the lamp off, collant circulated through the racks, thus cooling the specimens and resulting in the formation of dew. When the collant stopped circulating, the lamp came on and the dew evaporated from the specimens. To insure increased thermal conductivity between test specimens and racks, silicone paste was applied to the backsides of most specimens. The paste also served to hold the specimens in place and protect the backsides from exposure.

Automatic instrumentation independently controlled the concentrations of the gaseous pollutants within each chamber. Air temperature and relative humidity were controlled prior to flowing into the chambers. During the dew/light cycle, however, both the air temperature and relative humidity fluctuated in the chambers.

EVALUATION OF THE SYSTEM

Results of a statistically designed controlled-environment experiment will only be as good as the controls. Thus, variability from the desired

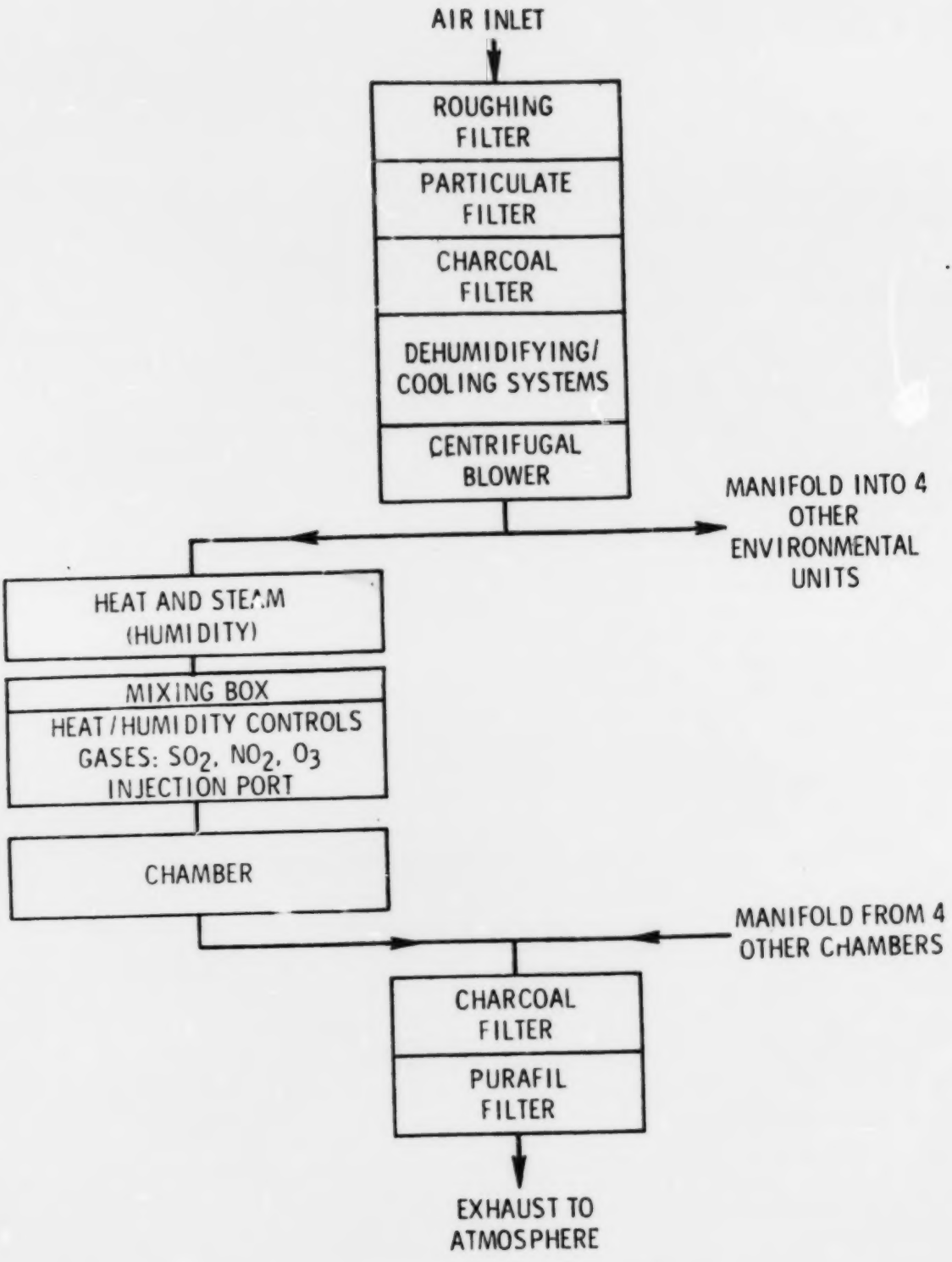

Figure 1. Environmental system flow diagram.

levels of pollutants, temperature, relative humidity, and light energy should be minimized. Statistical techniques were used to determine which parts of the system needed adjustment.

Chamber Lighting

The energy distribution from the xenon lamp within each chamber was measured and recorded as millivolts by a Talley Industries SOL-A-Meter. The distribution of energy on the specimen racks within the five chambers was balanced by (1) varying the lamp wattage, (2) placing reflectors in the light cap, (3) varying the angle of the specimen rack, and (4) reducing the reflectivity of the walls with a light spray of flat black paint.

An analysis of variance (Table 2) was carried out on the energy data to determine chamber and position effects. The calculated F statistic (Table 1) revealed that chamber differences were statistically insignificant. The position effect, however, was significant at the 5 percent probability level. Best estimate of the overall mean energy ($\bar{x}$) was 61.51 millivolts with a standard deviation (2S) of 3.38 for 89 degrees of freedom. The coefficient of variation was 3 percent. With these tolerance limits it was 95 percent certain that less than a 6.8 percent variation from the mean energy existed for 95 percent of the measurements. This relatively small amount of variability did not warrant the stratification of position as a variable. Placing the material test specimens randomly within each chamber minimized any bias that could have been caused by the position effect.

Table 2. ANALYSIS OF VARIANCE OF XENON LAMP ENERGY DATA

Source	Sum of squares	Degrees of freedom	Mean squares	F_{calc}	F_{table}[a]
Position	55.5960	17	3.2704	2.05	1.76
Chamber	5.7005	4	1.4251	1.09	2.50
Residual[b]	89.0596	68	1.3097		
Total	150.3560	79	1.6894		

[a] 5 percent probability level.

[b] Residual was confounded with a possible chamber x position interaction effect because the experiment was not replicated. It was taken as the error term in calculating the F values.

Chamber Pollutant Distribution

It is essential that the movement of polluted air be uniformly distributed across the test specimens. A plenum (sheet of stainless steel with 0.74-cm holes space 2.5 cm apart) was installed about 12.7 cm above the base of each chamber. The plenum created a pressure drop in the movement of air across it, thereby facilitating the mixing of pollutants within the chambers. The air flow from each chamber was measured in the exhaust ducts with a pitot tube. The air flow to each chamber was then balanced by means of a vane installed in the air supply duct.

To measure the distribution pattern of polluted air within the chambers, specimens of blue-colored test ribbon were placed at various locations within the chambers about 15.24 cm above the plenum and parallel to the air flow. The test ribbon was developed by the American Association of Textile Chemists and Colorists and is sensitive to NO_2. All five chambers were operated at constant conditions:

Temperature	35°C (95°F)
Relative humidity	5 percent
Nitrogen dioxide	940 $\mu g/m^3$
Air flow	2.7 m^3/min (2.5 air changes per minute)

After 48 hours exposure, the color of the ribbon specimens was measured photoelectrically with a Hunter Model D25A Color Difference Meter. The magnitude of the color change of each ribbon specimen was recorded as ΔE values. An analysis of variance (Table 3) was conducted to determine the significance of chamber and position effects.

Table 3. ANALYSIS OF VARIANCE OF POLLUTANT (NO_2) DISTRIBUTION WITHIN THE CHAMBERS

Source	Sum of squares	Degrees of freedom	Mean squares	F_{calc}	F_{table}[a]
Position	0.02344	8	0.00293	3.84	2.25
Chamber	0.00424	4	0.00106	1.40	2.67
Residual[b]	0.02441	32	0.00076		
Total	0.05209	44	0.00118		

[a] 5 percent probability level.

[b] Residual was confounded with a possible chamber x position interaction effect because the experiment was not replicated. It was taken as the error term in calculating F values.

The calculated F statistic (Table 3) for the pollutant distribution within the chambers indicated that the chamber effect was statistically insignificant; however, position effects existed at the 5 percent probability level. The best estimate of the overall mean ($\bar{x}$) for the ΔE values was 3.50 with a standard deviation (2S) of 0.069 for 8 degrees of freedom. The coefficient of variation was 1 percent. With these tolerance limits it was 95 percent certain that less than a 2.25 percent variation from the mean color change could be expected for 95 percent of the measurements. Again, randomly placing the test specimens within the chambers minimized bias that this variable could have caused.

Control Capability of Environmental Factors

Table 4 shows the control capability of the environmental factors--temperature, humidity, and pollutants--based on 24 hours continuous exposure and recording. The variability (2S) for the control capability of the

Table 4. CONTROL CAPABILITY OF ENVIRONMENTAL FACTORS WITHIN THE CHAMBERS

Environmental factors	Control point	Control Capability	
		$\bar{x}$	2S
Temperature, C°	35 (95°F)	34.8	±2
Humidity, %	90	88.8	±2.2
	50	50.4	±1.1
Ozone, $\mu g/m^3$	980	991.8	±31.4
	196	199.9	±11.8
Sulfur dioxide, $\mu g/m^3$	1310	1372.9	±131.0
	262	275.1	±23.6
Nitrogen dioxide, $\mu g/m^3$	940	930.6	±26.3

environmental factors appeared to be proportional to some function of level ($\bar{x}$). Such a relationship is not uncommon and is frequently encountered in controlled experimentation. It posed no problems in computations using exposure data.

The control of temperature and relative humidity was within the mixing box prior to the air entering the environmental chambers. During the dew/light

cycle, the temperature and relative humidity were not controlled but allowed to fluctuate in the chambers. The three gaseous pollutants were injected into the mixing box but were controlled within the chambers. Air samples were continuously taken from each of the chambers by means of a manifold system connected to a monitoring analyzer. The monitoring analyzers were specific for measuring concentrations of each of the three pollutant gases. The levels of the pollutants were constant during the dew/light cycle.

SECTION VI

STUDY DESIGN

The overall study was a first-cut attempt to determine under simulated conditions the effects on materials of three gaseous pollutants for which national ambient air quality standards have been established. To accomplish this goal, a statistical experimental design was chosen to provide data for assessing both direct and synergistic effects.[3] Parameters selected and incorporated into the experimental design included materials for exposure, environmental factors (temperature, humidity, pollutants), and levels of control.

SELECTION OF MATERIALS

In prior years, EPA sponsored state-of-the-art surveys to gather technical and economic information concerning the effects of air pollution on material products. A systems approach study,[4] prepared by Midwest Research Institute (MRI), ranked materials according to potential economic damage by gaseous air pollution. Table 5 summarizes the results of the ranking by generic classes of materials.

Table 5. RANKING OF MATERIALS ACCORDING TO ESTIMATED DAMAGE BY GASEOUS POLLUTANTS

Materials	Dollar loss, percent of total	Number of references with useful information
Metals	39	54
Paints	32	7
Textiles	9	14
Elastomers	5	12
Plastics	3	9
All others	12	4

The potential economic loss for pollutant-damaged metals ranked higher than other materials; published information was also highest. Damage to paints ranked second in economic importance. Equally significant, the MRI study revealed that only a small amount of published information was available on the effects of air pollutants on paints and other non-metallic materials.

Using the MRI study as a guide, one or more materials from each generic class were selected for the exposure study. Table 6 lists these materials; they all represent large sales volume and therefore are commercially important.

Table 6. MATERIALS SELECTED FOR THE CHAMBER EXPOSURE STUDY

Metals	Weathering steel, galvanized steel, aluminum alloy
Paints	Oil base house paint, acrylic latex house paint, vinyl coil coating, acrylic coil coating
Textiles	Dyed drapery fabrics
Elastomers	White sidewall rubber from a radial ply tire
Plastics	Vinyl house siding
Stone	White Cherokee marble
Cement	Portland

STATISTICAL DESIGN OF EXPOSURE EXPERIMENT

A statistically designed exposure experiment must include environmental factors that are most likely to affect the service life of materials. Environmental factors known to affect materials during exposure are sunlight (ultraviolet radiation), relative humidity, temperature, dew, and pollutants. Other environmental factors such as snow and frost occur infrequently with seasonal changes and are difficult to simulate in controlled environmental chambers. Of the gaseous pollutants for which national ambient air quality standards have been set, sulfur dioxide (SO_2), nitrogen dioxide (NO_2), and ozone (O_3) are known to affect different materials during their expected service life. As many of these environmental factors as possible, therefore, should be incorporated into a statistically designed experiment.

Although numerous statistical plans for conducting experiments and collecting data are available, a two-level factorial arrangement was selected because it is an excellent method for identifying the environmental factors or combination of factors, or both, that produce significant effects (materials damage). Table 7 presents the environmental factors and exposure levels selected. The low levels for the three gaseous pollutants represent the national primary ambient air quality standards, whereas the high levels represent concentrations that can exist at industrial sites. Levels selected for temperature and relative humidity are not extreme conditions and are frequently recorded. In this experimental model, the factors are thus fixed.

Table 7. ENVIRONMENTAL FACTORS AND LEVELS USED IN THE CHAMBER EXPOSURE EXPERIMENT

Environmental factors	Levels	
	Low	High
Sulfur dioxide, $\mu g/m^3$	79	1310
Nitrogen dioxide, $\mu g/m^3$	94	940
Ozone, $\mu g/m^3$	157	980
Temperature, C°	13	35
Relative humidity, %	50	90

In addition to the environmental factors, the total time of exposure and the time frame of each dew/light cycle were constant for each environmental condition. Total exposure duration was 1000 hours; however, materials were also evaluated after exposure periods of 250 and 500 hours. Each dew/light cycle lasted 40 minutes and consisted of 20 minutes of darkness and subsequent formation of dew, and 20 minutes of simulated sunlight.

Since there are five factors at two levels, the complete experimental design called for 32 (2^5) difference environmental exposure conditions--one at each combination of factor and level (Table 8)--and did not include replication of each exposure condition. The large number of exposure conditions was necessary because of the many direct and synergistic or interaction effects that may occur. On the other hand, the probability that all of these effects would actually occur was quite small. Since each exposure condition was to be 1000 hours, it was more practical to perform fewer exposures. Therefore, 16 exposure conditions (represented by X_1 through X_{16} in Table 8) were selected initially. These exposure conditions included the direct and interaction effects of the three gaseous pollutants and relative humidity at the high temperature level. The high temperature level was selected because, according to reaction kinetics, environmental factors that are statistically insignificant at high temperatures will most likely show insignificant interactions with temperature. Thus, the results of the first 16 high temperature exposures would determine which, if any, of the low temperature exposures (X_{17} - X_{32}) should be conducted. Furthermore, the chances were good that the low temperature exposures would not be necessary to identify environmental factors that cause significant effects. For similar reasons, the sequential performance of exposures was structured rather than randomized. (If effects could not be observed at high levels, there would be no need to study low levels.) Possible bias introduced by this procedure was minimized by the type of F-test used in the analysis of data.

Table 8. TWO-LEVEL FACTORIAL ARRANGEMENT

High relative humidity		Low relative humidity		Exposure condition		
High Temperature	Low Temperature	High Temperature	Low Temperature			
X_1	X_{17}	X_2	X_{18}	Low SO_2	Low O_3	Low NO_2
X_3	X_{19}	X_4	X_{20}	High SO_2		
X_5	X_{21}	X_6	X_{22}	Low SO_2	High O_3	
X_7	X_{23}	X_8	X_{24}	High SO_2		
X_9	X_{25}	X_{10}	X_{26}	Low SO_2	Low O_3	High NO_2
X_{11}	X_{27}	X_{12}	X_{28}	High SO_2		
X_{13}	X_{29}	X_{14}	X_{30}	Low SO_2	High O_3	
X_{15}	X_{31}	X_{16}	X_{32}	High SO_2		

TREATMENT OF DATA

Statistical analysis of variance was applied to the exposure data for each material. With the two-level factorial experiment, it was possible to determine which of the 15 direct and interaction factors had a statistically significant effect on selected material properties (corrosion rates, erosion rates, color change, etc.). Since each exposure condition was not replicated, the inability to precisely control the factors may have biased the analysis of variance because it could not be included in the calculation of error variability. The error term included only within-chamber-variability caused by position and time effects and possibly non-linearity of the time-damage function.

If a factor (one of 15 direct or interaction factors) actually has no effect on a material, the calculated variability associated with that factor is caused by error. In non-replicated statistically designed experiments, it is often assumed that the highest order of interaction is the least likely

factor to cause an effect and the variability associated with it is used to calculate the error mean square. Risks, however, are involved in making this assumption. First, interactions may actually affect the response and, therefore, the resulting F test on other factors would be less sensitive. Second, in a two-level factorial arrangement only one degree of freedom is associated with an interaction factor; this renders the F test less sensitive than when using an error term with more degrees of freedom. With a less sensitive F test, error is more likely to mask the actual effects of tested factors.

The sensitivity of the F test can be improved by including in the error term other interaction factors that are not likely to have an effect on the response. Nevertheless, some degree of risk does exist, since the included factors may cause effects. The risk, however, is somewhat mitigated by averaging any effects with the error variability and by the increased number of degrees of freedom.

When applying the F test for significance in the analysis of variance of this study, the residual variability associated with all three and higher variable interaction factors was used to calculate the error mean square.

SECTION VII

MATERIALS TESTING TECHNIQUES AND EVALUATION

TESTING TECHNIQUES

Testing techniques to measure effects were selected to provide damage data that would reflect loss of service life. Table 9 summarizes the techniques used for each material. Later chapters, which present and discuss the exposure results for individual materials, give additional details on testing techniques.

Table 9. MATERIALS TESTING TECHNIQUES

Material	Testing technique
Weathering steel	Gravimetric (loss-in-weight).
Galvanized steel	Gravimetric (loss-in-weight).
Aluminum alloy	Time to failure (cracking) of stressed C-rings.
Paint	Gravimetric (loss-in-weight). Loss-in-film-thickness.
Dyed fabric	Color change. Microscopic examination of fibers.
Rubber tire	Loss-ir-breaking-strength of rayon cord reinforced white sidewall rubber. Length and depth of rubber cracking.
Plastic house siding	Visual appearance--cracks, discoloration, staining, etc.
Marble and cement	Gravimetric (loss-in-weight). Microscopic examination.

EVALUATION

Before conducting the exposure experiment, it was necessary to evaluate the techniques for measuring damage to materials and the effectiveness of the dew/light cycle in accelerating the damage. To assess these parameters, specimens of the selected materials were exposed for 1000 hours in two chambers receiving clean air at 35°C and 90 percent relative humidity. One chamber operated continuously on a 40-minute dew/light cycle; the other operated at constant temperature and relative humidity (no dew/light cycle).

The galvanized steel and paint panels were evaluated for loss-in-film-thickness after exposure periods of 250, 500, and 1000 hours. The method of least squares was used to statistically analyze the rate of loss-in-film-thickness for these materials Tables 10 and 11 present the results from the two chamber exposure conditions.

Table 10. RATE OF LOSS-IN-FILM-THICKNESS DURING THE DEW/LIGHT CYCLE EXPOSURE CONDITION

Material	Number of observations	Rate of loss-in-film-thickness, μm/yr	95% conf. limits, μm/yr
Galvanized steel	36	0	
Acrylic coil coating	90	6.13	± 1.49
Vinyl coil coating	90	4.15	± 3.03
Oil base paint	36	267.	± 484
Latex paint	36	25.9	± 39.0

Table 11. RATE OF LOSS-IN-FILM-THICKNESS DURING THE CONSTANT TEMPERATURE AND RELATIVE HUMIDITY EXPOSURE CONDITION

Material	Number of observations	Rate of loss-in-film-thickness, μm/yr	95% conf. limits, μm/yr
Galvanized steel	36	0	
Acrylic coil coating	90	10.37	± 0.56
Vinyl coil coating	90	6.15	± 1.91
Oil base paint	36	32.9	± 49.4
Latex paint	36	0	

After a small initial loss, the galvanized steel panels exposed in both chambers had zero loss rates. An initial zinc loss of 4.40 ± 1.30 μm was recorded for the dew/light cycle condition, whereas for the constant temperature-relative humidity condition, 0.42 ± .93 μm was initially lost. For the exposed paint specimens, the dew/light cycle accelerated the rate of loss-in-film-thickness for the oil base and latex house paints, but not the two coil coatings. This anomaly may have been caused by the lack of experimental replication; however, it was more likely caused by inaccuracy of the measurement technique. Film thickness was measured using a Dermitron instrument, an electronic non-destructive thickness tester engineered to produce direct thickness reading of metallic and non-conductive coatings on steel and non-magnetic metals. Gravimetric analysis was later used in conjunction with film thickness measurements.

Tensile strengths (psi) of the rayon cord reinforced rubber tire specimens were measured after the 1000-hr exposure period for both environmental conditions. An analysis of variance (Table 12) was made on the breaking strength data to determine significant effects. The calculated F statistic revealed that

Table 12. ANALYSIS OF VARIANCE FOR RAYON TIRE CORD BREAKING STRENGTH

	Sum of squares	Degrees of freedom	Mean squares	F calc.	F table
Chamber	9894.4	1	9894.4	21.75*	5.32
Stress**	3369.8	1	3969.8	7.41	5.32
Chamber x Stress	965.7	1	965.7	2.12	5.32
Error***	3639.5	8	454.9		
Total	17869.4	11			

* Exceeds the 5 percent probability value

**Rubber strips were stretched 10 and 20 percent

*** Replication error

the chamber and stress effects were statistically significant at the 5 percent probability level. However, the interaction effect of chamber x stress was insignificant. In contrast to these results, no significant difference was found in the breaking strength of the white sidewall rubber (after the

reinforcing cord had broken) exposed to the two chamber conditions. Since the exposure conditions affected the cord strength but not the rubber, and since the rubber protected the cord from damage by light from the xenon lamp, the cord effect must have been a result of differences in moisture content. The strength of rayon generally decreases with an increase in moisture content. By means of absorption and wicking action, moisture entered the exposed ends of the rayon cord in the tire specimens. To prevent this action in subsequent exposures, the ends of rubber tire specimens were dipped in wax.

The dew/light cycle accelerated the weathering of the remaining exposed materials. Measurement techniques for these materials provided damage data for which significant differences were distinguished. As a result, no additional techniques were needed to assess damage of these materials.

SECTION VIII

EFFECTS ON WEATHERING STEEL

Weathering steel was developed for use in unpainted exterior architectual designs. In most environments, the steel develops a small grained strongly adherent rust coating that tends to serve as a protection film against subsequent corrosion. Weathering steel has been used in the design and construction of the Chicago Civic Center, the Washington Battelle Memorial Institute Building, and the New York Ford Foundation Office.

METHODOLOGY

The weathering steel exposed in this study was Cor-Ten A, a product of United States Steel Corporation. Table 13 gives the elemental analysis of Cor-Ten A. The measured yield point and ultimate tensile strength were 35,820 N/cm^2 and 54,480 N/cm^2, respectively.

Table 13. ELEMENTAL ANALYSIS OF WEATHERING STEEL

Elemental Composition, %								
C	Mn	P	S	Si	Cu	Ni	Cr	Fe
0.11	0.37	0.10	0.018	0.39	0.29	0.11	0.90	Remainder

Corrosion rates of most metals normally accelerate when metals are exposed to polluted environments. The rate of corrosion, therefore, was selected as the means for assessing the effects produced by the various controlled environment exposure conditions. Corrosion was measured by the weight-loss method. This method consisted of weighing the panel before exposure, and removing the corrosion products and reweighing after exposure. The difference in weight was a measure of the amount of metal that corroded during the exposure period.

Panels measuring 7.6 cm x 12.7 cm were sheared from sheet stock. The panels were cleaned by scrubbing them in a warm detergent solution followed by separate rinses in distilled water and acetone. They were then weighed on an analytical balance to within $\pm$ 0.1 mg.

Six panels were exposed to each of the 16 polluted and 4 clean air conditions. The panels were randomly placed on chamber exposure racks and two panels were randomly removed after nominal exposure periods of 250, 500, and 1000 hours.

Corrosion products on the exposed panels were chemically removed by immersion for one hour or longer in Clark's solution[5], followed by scrubbing and final rinses in distilled water and acetone. The panels were then weighed, the weights corrected for the loss of base metal [0.06 g/ (panel hr.)] while in Clark's solution, and weight-loss values calculated. To render the weight-loss values (g/panel) more meaningful, they were converted to equivalent thickness-loss values (μm) by using the factor 13.345 μm/g.

RESULTS AND DISCUSSION

Corrosion of weathering steel is normally a parabolic function of time. The corrosion data collected in this study, however, were essentially linear with time. The relatively short exposure periods (1000 hrs.) probably accounted for the deviation.

Because of the linear relationship, a mean corrosion rate for each exposure condition was calculated using the method of least squares through the origin. Tables 14 and 15 present individual corrosion rates for the polluted air and clean air exposures, respectively. Corrosion rates in polluted air ranged from 84 to 762 μm/yr with an average of 383 μm/yr. Best estimate of the standard deviation on individual corrosion rates in polluted air was ± 72 μm/yr. Clean air corrosion rates ranged from 1 to 86 μm/yr. The highest clean air corrosion rate was about the same as the lowest rate in polluted air.

Table 14. CORROSION RATES OF WEATHERING STEEL EXPOSED TO DESIGNATED CONTROLLED POLLUTED AIR ENVIRONMENTAL CONDITIONS

Corrosion rate and standard deviation, μm/yr				Exposure condition	
High relative humidity		Low relative humidity			
High SO_2	Low SO_2	High SO_2	Low SO_2		
753 ± 85	256 ± 27	414 ± 151	179 ± 30	High O_3	High NO_2
762 ± 121	178 ± 44	607 ± 105	162 ± 62	Low O_3	
736 ± 90	230 ± 27	479 ± 78	123 ± 26	High O_3	Low NO_2
656 ± 56	147 ± 13	371 ± 18	84 ± 14	Low O_3	

Note: Corrosion rates based on six data sets per exposure condition.

Table 15. CORROSION RATES OF WEATHERING STEEL EXPOSED TO DESIGNATED CONTROLLED CLEAN AIR ENVIRONMENTAL CONDITIONS

Corrosion rate and standard deviation, μm/yr		
High relative humidity	Low relative humidity	Temperature
86 ± 31	28 ± 10	35°C
1.03 ± 0.17	1.07 ± 0.06	13°C

Note: Corrosion rates based on six data sets per exposure condition.

Tables 16 and 17 show analyses of variance of the experimental data for the polluted and clean air exposure conditions, respectively. On the basis of calculated F values, the important factors controlling corrosion were concentration of SO_2, relative humidity, and temperature. The interaction between SO_2 and relative humidity was significant at a lower confidence level.

As shown in previous studies[6,7], electrolytic corrosion occurs only when metal panels are wet. During dew/light cycles in the chambers, panel temperatures continually varied, thus causing changes in relative humidity adjacent to the panels. When temperatures were below the dew point, moisture condensed on the panels. Because of the hygroscopic nature of corrosion products, panels also became moist even at temperatures above the dew point.

Thermocouples attached to panels were used to monitor panel temperatures during the dew/light cycles for each clean air exposure condition. Figure 2 shows the results. Theoretically, the critical factors controlling corrosion are the time-of-panel-wetness and the geometric mean temperature during the time panels are wet. Since the moisture content of the air entering the chambers was essentially constant (set by the input conditions), time-of-panel-wetness per cycle was estimated by using the cycling temperature data to calculate relative humidity values (adjacent to panels) as a function of time. Visual observations, however, detected moisture on panels at a calculated relative humidity of about 85 percent. This was probably due to the hygroscopic nature of the corrosion products. Thus, panels were considered wet at temperatures corresponding to relative humidities equal to or greater than 85 percent. Table 18 shows the calculated times-of-panel-wetness per dew/light

Table 16. ANALYSIS OF VARIANCE OF WEATHERING STEEL CORROSION DATA FOR POLLUTED AIR EXPOSURE CONDITIONS

Factor	Contrast	Sum of squares	Degrees of freedom	Mean square	F	R^2
SO_2	213.7	730726	1	730726	258.11**	0.790
RH	12.7	105138	1	105138	37.14**	0.114
O_3	12.7	2590	1	2590	0.91	0.003
NO_2	30.4	14810	1	14810	5.23	0.016
SO_2 x RH	48.3	37264	1	37264	13.16*	0.040
SO_2 x NO_2	-14.4	3322	1	3322	1.17	0.004
SO_2 x NO_2	6.5	673	1	673	0.24	0.001
RH x O_3	16.3	4231	1	4231	1.49	0.005
RH x NO_2	-7.8	975	1	975	0.34	0.001
O_3 x NO_2	-26.1	10870	1	10870	3.84	0.012
Residual		14155	5	2831		0.003
Total		924754	15			

Notes: F uses the residual mean square in the denominator

R^2 is the coefficient of determination excluding the within chamber variability

** 99 percent probability level of significance

* 95 percent probability level of significance

Table 17. ANALYSIS OF VARIANCE OF WEATHERING STEEL CORROSION DATA FOR CLEAN AIR EXPOSURE CONDITIONS

Factor	Contrast	Sum of squares	Degrees of freedom	Mean square	F	R^2
RH	14.49	839.8404	1	839.8404	3.24	0.085
Temperature	27.75	3080.2550	1	3080.2500	11.89**	0.310
RH x T	14.51	842.1604	1	842.1604	3.25	0.085
Error		5181.7875	20	259.0894		0.521
Total		9944.0383				

** 99 percent probability level of significance

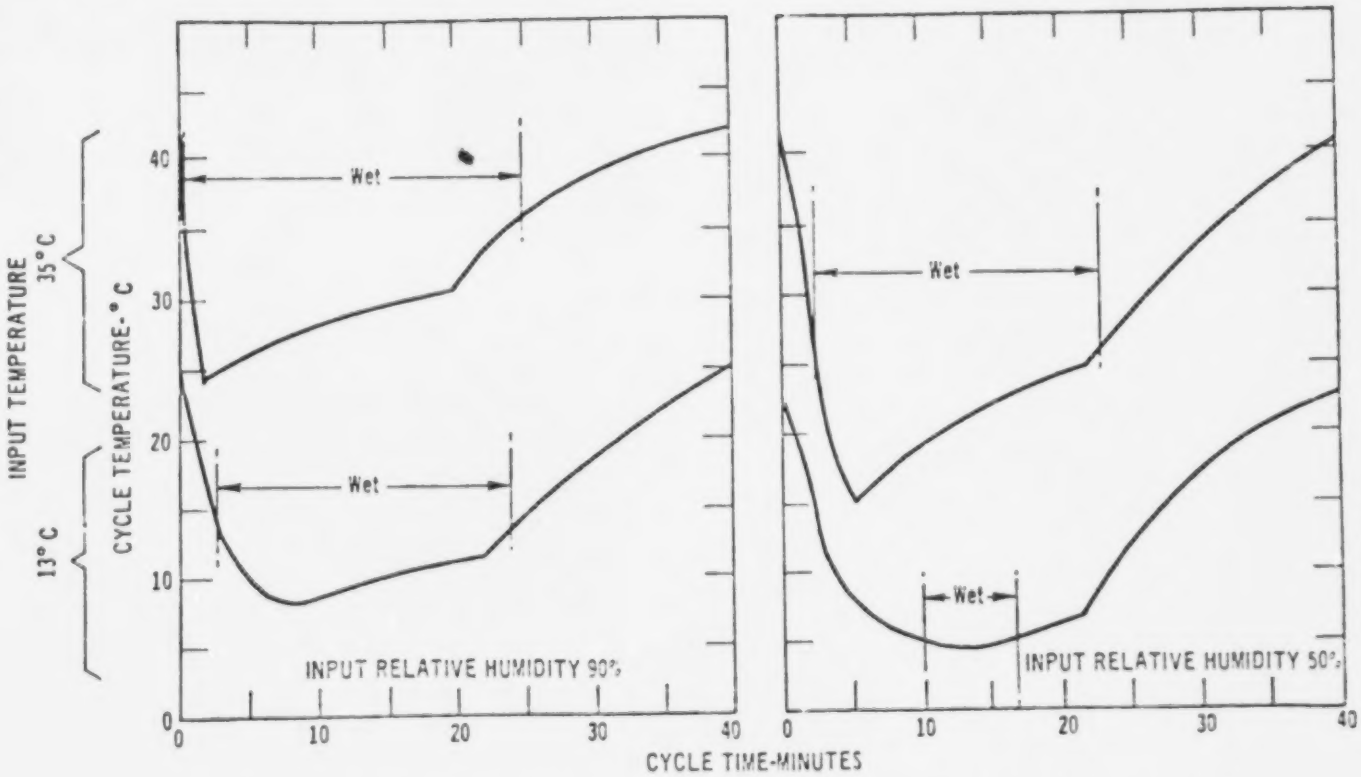

Figure 2. Temperature-time profiles for exposed metal panels during chamber dew/light cycles.

Table 18. TIME-OF-PANEL-WETNESS PER DEW/LIGHT CYCLE AND GEOMETRIC MEAN PANEL TEMPERATURE WHEN WET AS A FUNCTION OF INPUT TEMPERATURE AND RELATIVE HUMIDITY

Input temperature	Input relative humidity	
	90%	50%
35°C	24.5 min 29.4°C	20.7 min 20.4°C
13°C	22.0 min 10.2°C	7.0 min 4.6°C

Note: Calculated values are for both weathering steel and galvanized steel.

cycle and geometric mean temperatures of panels when wet for each clean air exposure condition.

Because steel corrodes only when wet, the corrosion data were analyzed in terms of the expected times-of-wetness. On the basis of long term atmospheric corrosion studies[8,9], the corrosion-time function should be more nearly parabolic than linear as was observed in the short term chamber exposures. In the clean air exposures, the reactants (steel, water, and oxygen) were present in excess and the reaction rate should be activation controlled. Thus, the theoretically expected relationship between corrosion, time, and temperature should be:

$$\ell n \frac{Corr}{\sqrt{t_w}} = \ell n \ a_o - \frac{E}{RT} \qquad (1)$$

where: Corr = thickness-loss, um
t_w = time-of-wetness, yr
E = activation energy, cal/(g-mol °K)
R = gas constant, 1.9872 cal/g-mol
T = geometric mean temperature of panels when wet, °K
a_o = regression coefficient

A least squares fit of the clean air experimental data resulted in

$$\ell n \frac{Corr}{\sqrt{t_w}} = 55.44 - \frac{31150}{RT} \quad (2)$$

or

$$Corr = \sqrt{t_w} \; e^{(55.44 - \frac{31150}{RT})} \quad (3)$$

This empirical function accounted for 92 percent of the variability in the clean air experimental data.

The reaction of steel with moisture and oxygen occurs with or without SO_2 present. Thus, the contribution of moisture and oxygen to the total corrosion may be excluded when analyzing the direct and synergistic effects of SO_2. This amount of corrosion, therefore, was calculated and substracted from each corresponding data set from the polluted air exposures and the resulting data fitted to the relationship:

$$\ell n \frac{Corr}{\sqrt{t_w}} = \ell n \, a_o + a_1 \, \ell n \, SO_2 - \frac{E}{RT} \quad (4)$$

where: Corr = thickness-loss, μm
t_w = time-of-panel-wetness, yr
SO_2 = concentration of SO_2, $\mu g/m^3$
E = activation energy, cal/(g-mol °K)
R = gas constant, 1.9872 cal/g-mol
T = geometric mean panel temperature when wet, °K
a_o, a_1 = regression constants

The calculated constant, $\frac{E}{R}$, was small, positive, and statistically insignificant. This fact strongly suggested that the reaction of SO_2 with steel was diffusion controlled rather than activation controlled. The coefficient for $\ell n \, SO_2$ was not statistically different from 0.5; corrosion, therefore, appeared to be proportional to $\sqrt{SO_2}$. Thus, the weathering steel experimental data were re-evaluated as a function of the square root of the dose, $\sqrt{t_w SO_2}$, and the resulting best fit of the theoretically consistent relationship was:

$$Corr = [5.64 \sqrt{SO_2} + e^{(55.44 - \frac{31150}{RT})}] \sqrt{t_w} \quad (5)$$

This empirical function accounted for 91 percent of the variability in the experimental data from both the clean and polluted air exposure conditions.

Figure 3 shows a plot of predicted versus experimental data. The deviation at the high end of the graph is probably because the experimental data were more consistent with a linear-time function than a parabolic-time function.

A better test of an empirical function is to determine how accurately it predicts actual long term atmospheric corrosion results. Fortunately, corrosion data for a similar weathering steel are available from a field study conducted in eight cities.[8] Although time-of-panel-wetness and temperature during time-of-wetness were not measured in the field study, average temperature and relative humidity during the total time of exposure were calculated. Thus, if relationships between average relative humidity and time-of-panel-wetness, and between average temperature and geometric mean temperature when panels are wet can be obtained, the empirical function may be expressed in terms suitable for making comparisons with the field data.

Guttman[7] has plotted the probable time-of-wetness as a function of relative humidity for both groundward and skyward surfaces of exposed metal panels. Assuming the average probability for the two surfaces represents the fraction of the total time panels are wet, the data fit a relationship

$$f_w = e^{4.04 - \frac{404}{RH}} \qquad (6)$$

where: f_w = fractional time-of-panel-wetness
RH = relative humidity, %

On the basis of the temperature cycle data in Figure 2, the geometric mean panel temperature when wet was about 6°K less than the average panel temperature for the total time of exposure. This information together with the field study data, were used to calculate factors (Table 19) that affected the atmospheric corrosion of weathering steel in each city. Thus, these factors may be used in the empirical function to predict the amount of corrosion likely to develop in each city.

A measure of corrosion predictability is the coefficient of variation, R^2, between predicted and field study values. Values of R^2 were calculated for each city of the field study; results are given in Table 20. With the exception of Los Angeles, predicted corrosion values agreed poorly with actual corrosion measured in cities with relatively high oxidant levels. The Los Angeles data was probably in good agreement because the low time-of panel-wetness did not allow much corrosion to develop, thus the magnitude of error was small. Regressions on the field data, however, strongly suggested that oxidants inhibited corrosion. The major oxidant in natural environments is ozone, but the chamber exposures showed that ozone produced neither inhibiting

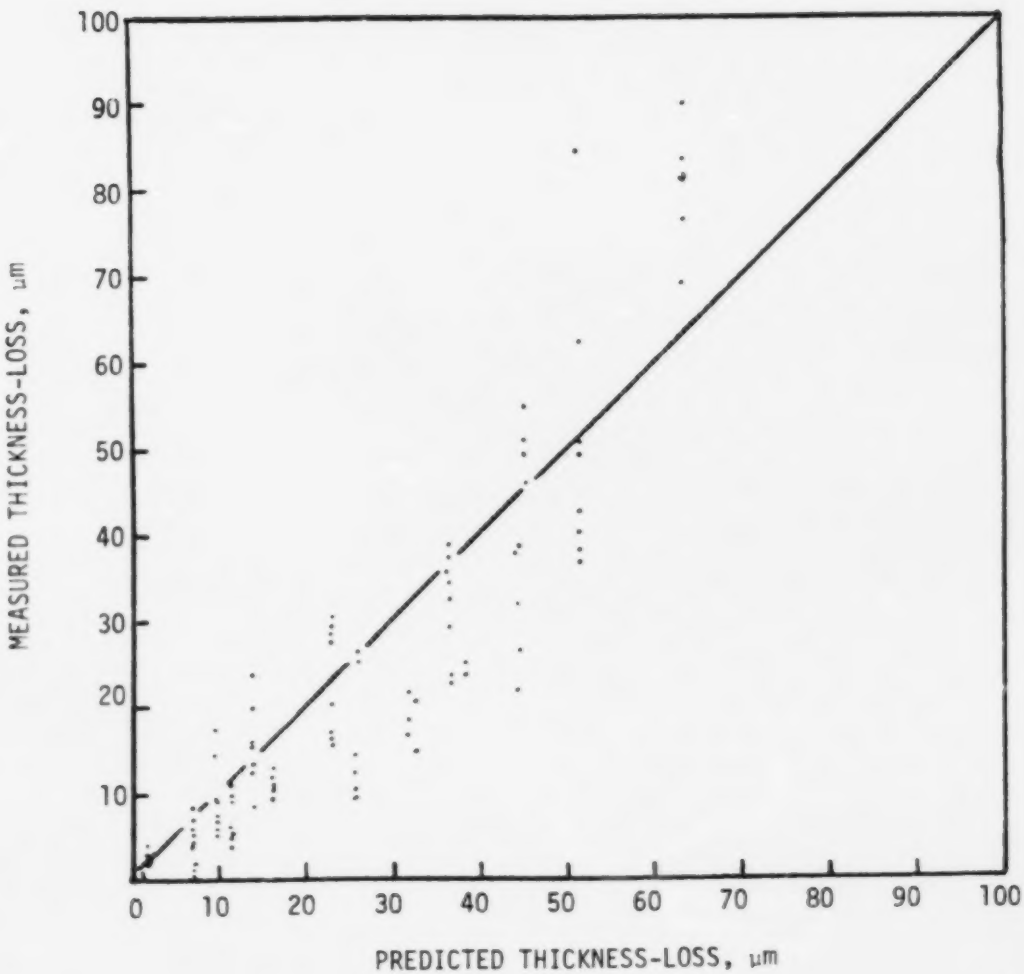

Figure 3. Comparison of predicted and measured thickness-loss values for weathering steel exposed to laboratory controlled polluted air and clean air conditions.

Table 19. FACTORS AFFECTING ATMOSPHERIC CORROSION OF WEATHERING STEEL EXPOSED AT URBAN SITES

City	Geometric mean panel temperature when wet, °K	Fractional time-of-panel-wetness, f_w	Average pollutant concentration, $\mu g/m^3$		Combined factor*
			SO_2	O_3	
Chicago	277.3	0.1136	406	47	38.42
Cincinnati	280.2	0.1628	79	59	20.47
Detroit	277.2	0.1367	118	24	22.77
Los Angeles	285.2	0.0841	39	75	10.68
New Orleans	287.5	0.2992	24	35	16.48
Philadelphia	279.1	0.1248	218	57	29.60
San Francisco	281.3	0.2244	34	37	15.94
Washington	281.0	0.0932	126	50	19.54

* $[5.64\sqrt{SO_2} + e^{(55.44 - \frac{31,150}{RT})}]\sqrt{f_w}$

Table 20. CORROSION PREDICTABILITY AS MEASURED BY COEFFICIENTS OF VARIATION, R^2, BETWEEN PREDICTED AND FIELD VALUES

City	Coefficient of variation, R^2, a measure of corrosion predictability
Chicago	0.976
Cincinnati	0.544
Detroit	0.997
Los Angeles	0.984
New Orleans	0.998
Philadelphia	0.392
San Francisco	0.978
Washington	0.701
Overall	0.846

nor accelerating effects. In the field study, some other oxidant, or unmeasured factor that was covariant with oxidant, apparently caused the inhibiting effect. Excluding the data from the high oxidant cities, the average coefficient of variation was 0.986. This was exceptionally good, expecially considering the simplifying assumptions that were made.

SECTION IX

EFFECTS ON GALVANIZED STEEL

Galvanized steel is widely used for such exterior applications as roofing, guttering, highway railing, and chain link fencing.

METHODOLOGY

Commercial grade 18 gauge galvanized steel sheet with an approximate 25 μm zinc coating was selected. The effects assessment method (weight-loss), panel size, pre-exposure cleaning procedure, and panel exposure sequence were the same as those used for the weathering steel.

Corrosion products on the exposed galvanized steel panels were chemically removed by immersion for about 10 minutes in a 10 percent aqueous ammonium chloride solution maintained at 72 to 80°C. The correction factor for zinc lost during chemical cleaning was 0.009 g/(panel min). Multiplying the corrected weight-loss values (g/panel) by 14.98 μm/g converted them to equivalent zinc film thickness-loss values (μm).

RESULTS AND DISCUSSION

As was theoretically expected, corrosion of the galvanized steel was essentially linear with time. Thus, an average corrosion rate for each of the 16 polluted air exposure conditions was calculated by the method of least squares through the origin. Table 21 shows the corrosion rates; they ranged from 3 to 33 μm/yr, and the best estimate of the standard deviation on individual rates was ± 5 μm/yr.

Corrosion rates for galvanized steel exposed to clean air conditions were unexpectedly high and have been presented and discussed as a separate publication.[10]

An analysis of variance (Table 22) was performed on the calculated polluted air corrosion rates. Both sulfur dioxide (SO_2) and relative humidity produced highly significant positive effects (99 percent probability level) on the corrosion rate of galvanized steel. Excluding within chamber error, these two factors accounted for 94 percent of the variability. Ozone also appeared to be a significant factor at the 95 percent probability level; however, it only accounted for about 3 percent of the variability. Therefore, it was not considered in further analysis of the data.

According to accepted corrosion theory, zinc surfaces corrode only when wet. Therefore, the data in table 21 may be reevaluated in terms of time-of-

Table 21. CORROSION RATES OF GALVANIZED STEEL EXPOSED TO DESIGNATED CONTROLLED POLLUTED AIR ENVIRONMENTAL CONDITIONS

Corrosion rate and standard deviation, μm/yr				Exposure Condition	
High relative humidity		Low relative humidity			
High SO_2	Low SO_2	High SO_2	Low SO_2		
33 ± 7.1	17 ± 5.2	19 ± 4.1	6.6 ± 0.9	High O_3	High NO_2
28 ± 1.5	12 ± 4.3	15 ± 2.1	3.8 ± 0.6	Low O_3	
29 ± 10	20 ± 11	17 ± 1.3	4.0 ± 0.9	High O_3	Low NO_2
25 ± 3.1	16 ± 6.6	16 ± 3.5	3.2 ± 2.1	Low O_3	

Note: Corrosion rates based on six data sets per exposure condition.

Table 22. ANALYSIS OF VARIANCE OF GALVANIZED STEEL CORROSION DATA FOR POLLUTED AIR EXPOSURE CONDITIONS

Factor	Contrast	Sum of squares	Degrees of freedom	Mean square	F	R^2
SO_2	6.2188	618.7781	1	618.7781	189.61**	0.484
RH	6.0272	581.2318	1	581.2318	178.10**	0.455
O_3	1.5893	40.4146	1	40.4146	12.38*	0.032
NO_2	-0.2644	1.1188	1	1.1181	0.34	0.000
SO_2 x RH	0.0565	0.0512	1	0.0512	0.02	0.000
SO_2 x O_3	0.1374	0.3022	1	0.3022	0.09	0.000
SO_2 x NO_2	-0.8088	10.4668	1	10.4668	3.21	0.008
RH x O_3	0.5486	4.8147	1	4.8147	1.48	0.004
RH x NO_2	0.3598	2.0714	1	2.0714	0.63	0.002
O_3 x NO_2	-0.4093	2.6806	1	2.6806	0.82	0.002
Residual		16.3176	5	3.2635		0.013
Total		1278.2478	15			

Notes: F uses the residual mean square in the denominator

R^2 is the coefficient of determination excluding the within chamber variability

** 99 percent probability level of significance

* 95 percent probability level of significance

panel-wetness and geometric mean panel temperature (Table 18) rather than total time. To convert to corrosion rates during time-of-panel-wetness, the corrosion results in Table 21 were divided by the time-of-wetness expressed as a fraction (0.6125 for high relative humidity and 0.5175 for low relative humidity).

The corrosion of galvanized steel should be consistent with the following theoretical relationship:

$$Corr = (a_o\ SO_2 + e^{\,b\ -\ E/RT})\ t_w \qquad (7)$$

where: Corr = zinc thickness-loss, μm
a_o,b = regression coefficients
SO_2 = SO_2 concentration, $\mu g/m^3$
t_w = time-of-wetness, yr
E = activation energy, cal/(g-mol °K)
R = gas constant, 1.9872 cal/g-mol
T = geometric mean temperature of panels when wet, °K

A best fit of the experimental data yielded:

$$Corr = (0.0187\ SO_2 + e^{\,41.85\ -\ 23240/RT})\ t_w \qquad (8)$$

This empirical function accounted for 91 percent of the variability in the experimental data from the polluted air exposure conditions. A comparison of the measured zinc thickness-loss values with predicted values is shown in Figure 4.

Previous research has shown that zinc corrodes more rapidly in urban and industrial areas than in rural areas.[11,12] Researchers suspect that atmospheric pollutants, especially sulfur dioxide, accelerate the corrosion of zinc by preventing the formation of a protective film, which probably consists of an insoluble zinc oxide and carbonate mixture. Several investigators have developed relationships between the amount of zinc corrosion and atmospheric concentration of sulfur dioxide.[7,13] The previous research, however, involved field exposures of high purity zinc panels to environmental factors that could not be controlled.

In the chamber study, galvanized steel panels were exposed to controlled levels of gaseous pollutants, temperature, and relative humidity. No attempt was made to remove oxygen or carbon dioxide from the air circulated through the chambers. These gases along with the pollutants were, therefore, readily available to react with the zinc coating during the time-of-panel-wetness.

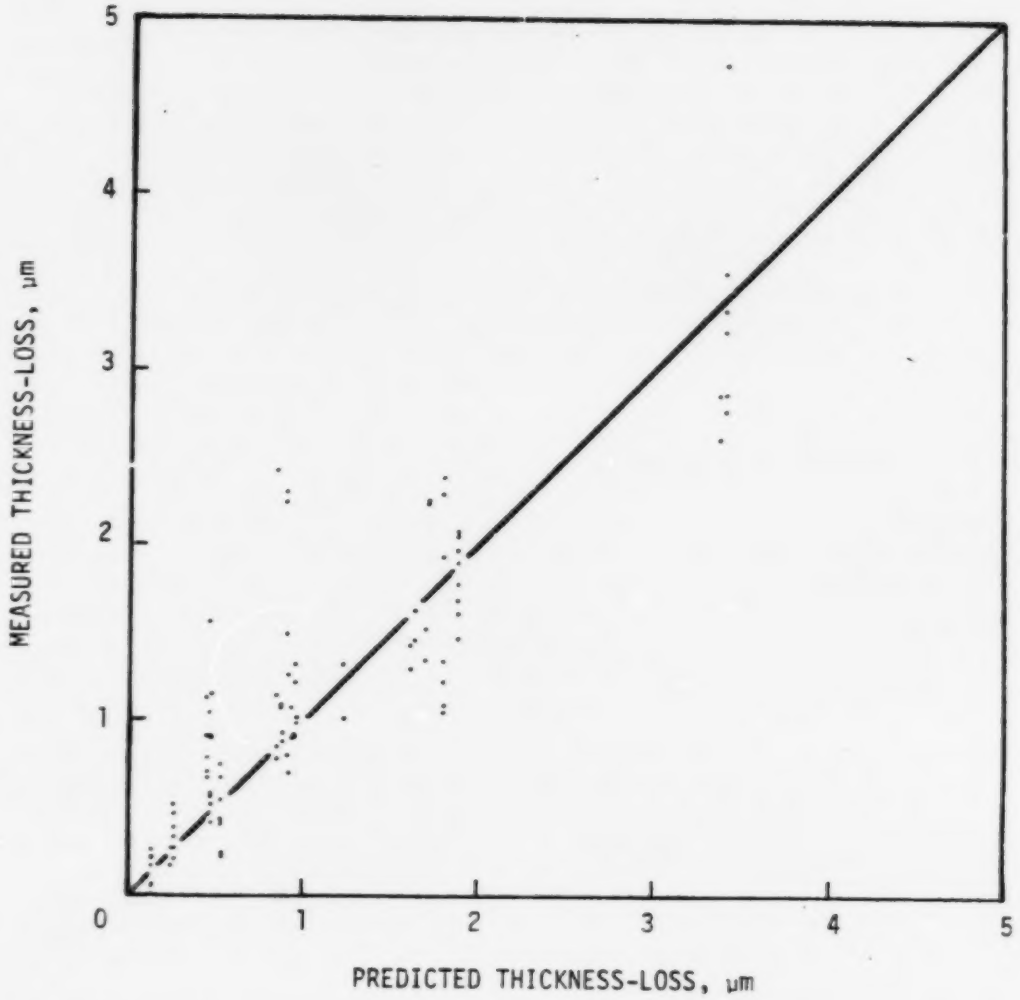

Figure 4. Comparison of predicted and measured thickness-loss values for galvanized steel exposed to laboratory controlled polluted air.

Two reactions are believed to occur simultaneously in the presence of the chamber pollutants: (1) the formation of zinc hydroxide or oxide, and (2) the formation of zinc sulfate. The analysis of variance of the chamber data, however, indicated that of the three gaseous pollutants, only sulfur dioxide significantly accelerated the corrosion rate. Therefore, the formation of sulfur containing corrosion products would be expected. Scanning electron photomicrographs of exposed panels (figure 5) revealed crystalline material uniformily dispersed over the zinc surface. X-ray diffraction patterns of the corrosion products were complex and indicated one or more unidentifiable hydrated compounds. Microprobe scans, however, revealed sulfur atoms, likely in the form of sulfate, to be uniformily distributed over the zinc surface.

During the dew cycle, the pH of the thin layer of condensate that formed on the galvanized panels was measured and found to remain acidic (pH of 5.6). However, the zinc corrosion products (oxides or hydroxides and sulfates) are known to be soluble in acidic media. Corrosion rates, therefore, should remain constant with time because the acidic dew not only dissolves the corrosion products but distributes them uniformily across the zinc surface (figure 5). The process continues during each cycle of dew formation.

The reactant (oxygen) producing the hydroxide or oxide was readily available during exposure; thus, the reaction with the zinc surface should be activation controlled. In comparison, sulfur dioxide levels were considerably lower; therefore, the formation of sulfate should be diffusion controlled. Carbon dioxide was also readily available to react with the zinc coating; however, the protective zinc carbonate film was not likely to form in the presence of an acidic (sulfurous acid) medium.

The best fit of the corrosion data produced an empirical function that accounted for 91 percent of the variability. Unfortunately, the predictability of this relationship cannot be tested because no comparable field data exist for exposed galvanized steel. However, field data for the corrosion of pure zinc panels are available.[13] After making minor tranformations in the empirical corrosion function, predicted corrosion values for galvanized steel were consistently lower than corrosion values for pure zinc measured during field exposures. The empirical function accounted for only 29 percent of the variability in the field data.

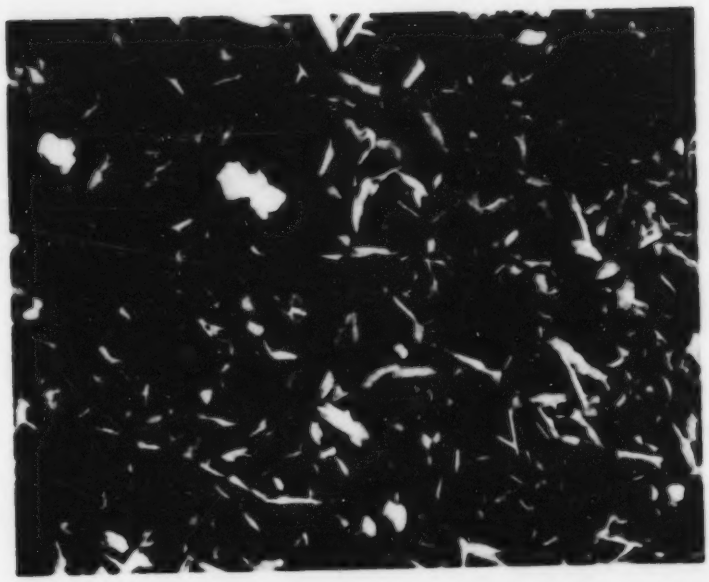

Figure 5. Scanning electron photomicrograph of an exposed galvanized steel panel showing uniformily dispersed crystalline material over the zinc surface.

SECTION X

EFFECTS ON ALUMINUM ALLOY

A number of catastrophic failures of metal structures, such as bridges, towers, and aircraft components, have been caused by a phenomenon called stress corrosion cracking. Broadly speaking stress corrosion cracking is a form of localized failure that is more severe under the combined action of stress and corrosion than would be expected from the sum of the individual effects of stress and corrosion acting alone. Failure is characterized by a brittle-type fracture in an otherwise ductile material. In some cases, the cause of failure has been linked to air pollution.

Several important alloys are susceptible to stress corrosion cracking. The most familiar example is brass which fails in environments containing ammonia. Investigators have found that a number of aluminum alloys also fail by stress corrosion cracking especially in seacoast environments. However, the 7000 series of high strength aluminum alloys, which contain little or no copper, is more susceptible to stress corrosion cracking in industrial environments than along the seacoast. Since air pollution is synonymous with industrial environments and is therefore a likely cause of failure, an alloy from this series was selected as a representative metal for assessing stress corrosion cracking.

METHODOLOGY

High strength aluminum alloy 7005-T53 was chosen for exposure. Table 23 gives the chemical analysis of this alloy. The main reason for choosing

Table 23. ELEMENTAL ANALYSIS OF ALUMINUM ALLOY 7005-T53

Elemental Composition, %										
Si	Fe	Cu	Mn	Mg	Cr	Ni	Zn	Ti	Zr	Al
0.09	0.22	0.04	0.40	1.58	0.09	<0.01	4.61	0.03	0.13	Remainder

this particular 7000 series alloy was that it was readily available as extruded tubing. This shape made it possible to easily fabricate C-ring test specimens, one of the common types of specimens used to assess stress corrosion.

The tubing had an outside diameter of about 5.7 cm with a wall thickness of about 0.23 cm. Fabricated C-ring specimens were 1.9 cm wide with machined edges; inside and outside surfaces remained as received.

C-ring specimens were stressed according to ASTM recommendations;[14] actual dimensions were measured to within 10 μm. Two levels of stress were used: 2.07×10^8 N/m^3 (30 ksi) and 2.76×10^8 N/m^3 (40 ksi). Figure 6 shows the design of a stressed C-ring specimen. To measure time-of-failure, each specimen was

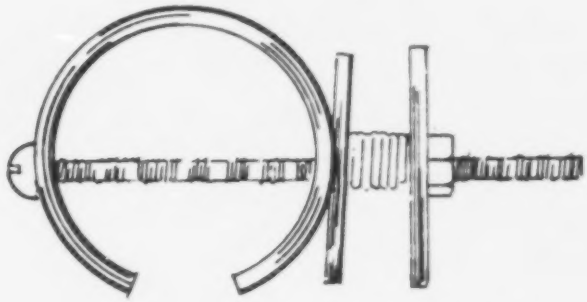

Figure 6. Method of stressing C-ring specimens

spring loaded and electrically connected to a recorder. An insulated wire was attached across the compressed spring. Failure of a C-ring specimen caused the wire to break, thus signaling the time-of-failure.

To simplify the electrical wiring scheme, a group of three equally stressed C-ring specimens were mounted on a metal (aluminum alloy 6061-T6) plate that was then placed at random on a chamber exposure rack. For each exposure condition, two groups (one at each stress level) of three specimens were exposed.

Each group of three specimens was wired according to Figure 7 so that time-of-failure for each specimen could be determined by recording step changes in voltages on a ten channel multipoint recorder. The resistance R in figure 7 was varied from one group to another to separate voltage traces on the recorder. Resistance values ranged from 0 to 35 Ω. When a specimen breaks, the recorded voltage increases and thus marks the time-of-failure.

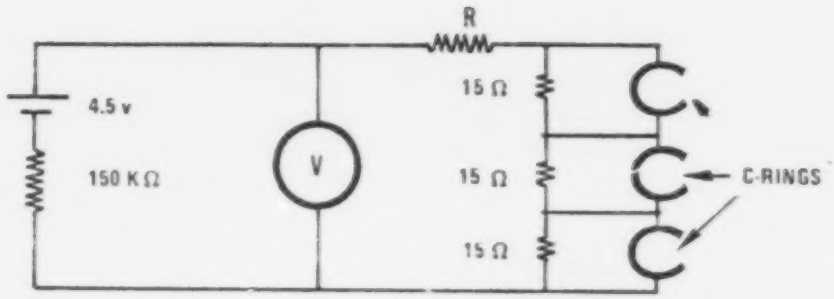

Figure 7. Wiring of specimens to record times-of-failure

RESULTS AND DISCUSSION

None of the specimens exposed for 1000 hours to the 16 polluted air environment conditions completely failed; thus, time-to-failure could not be used as a response.

Specimens developed small intergranular cracks perpendicular to the stress direction (Figure 8). From a visual standpoint, number and lengths of these cracks appeared to be a function of exposure time, severity of the environment, and level of stress.

Selected specimens were examined by both light and scanning electron microscopy. The cracks were intergranular and microprobe analysis revealed sulfur on the fracture faces (Figure 9).

A 5.1 cm cord across the stressed area was cut from each C-ring specimen after 1000 hours exposure, and compressed to failure by bending in a tensile-compression testing instrument. The maximum load required to bend the specimen was assumed to be a function of the remaining uncracked cross sectional thickness and was recorded as the response to the controlled environmental factors. A typical load-deflection curve on these specimens had two maxima. The first represented buckling and the second bending; the second maximum was used as the response.

Results for the polluted air exposure conditions are given in Table 24 and ranged from a low of 288 N to a high of 804 N. Low values represent cross sections reduced by stress corrosion cracks. The best estimate of the standard deviation on any one set of data was ± 108 N.

Reproduced from
best available copy.

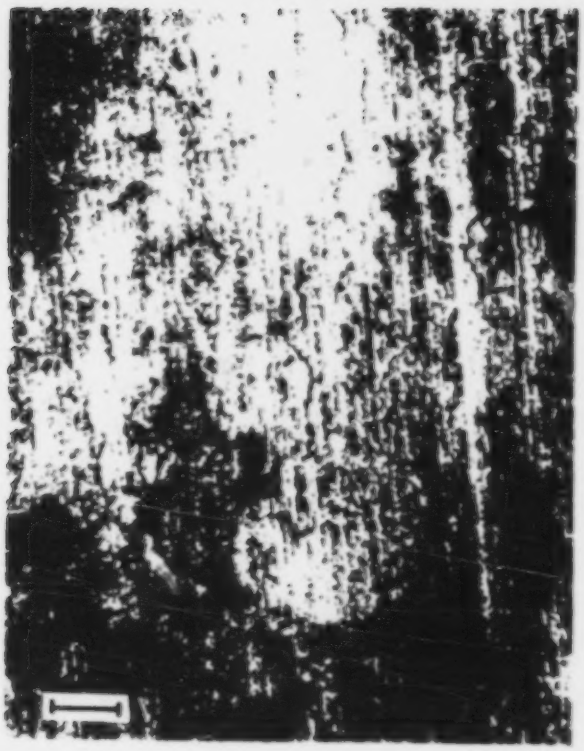

Figure 8. Stress induced integranular cracks in aluminum alloy 7005-T53 after 1000 hours exposure to air containing SO_2. (Mark = 1 mm)

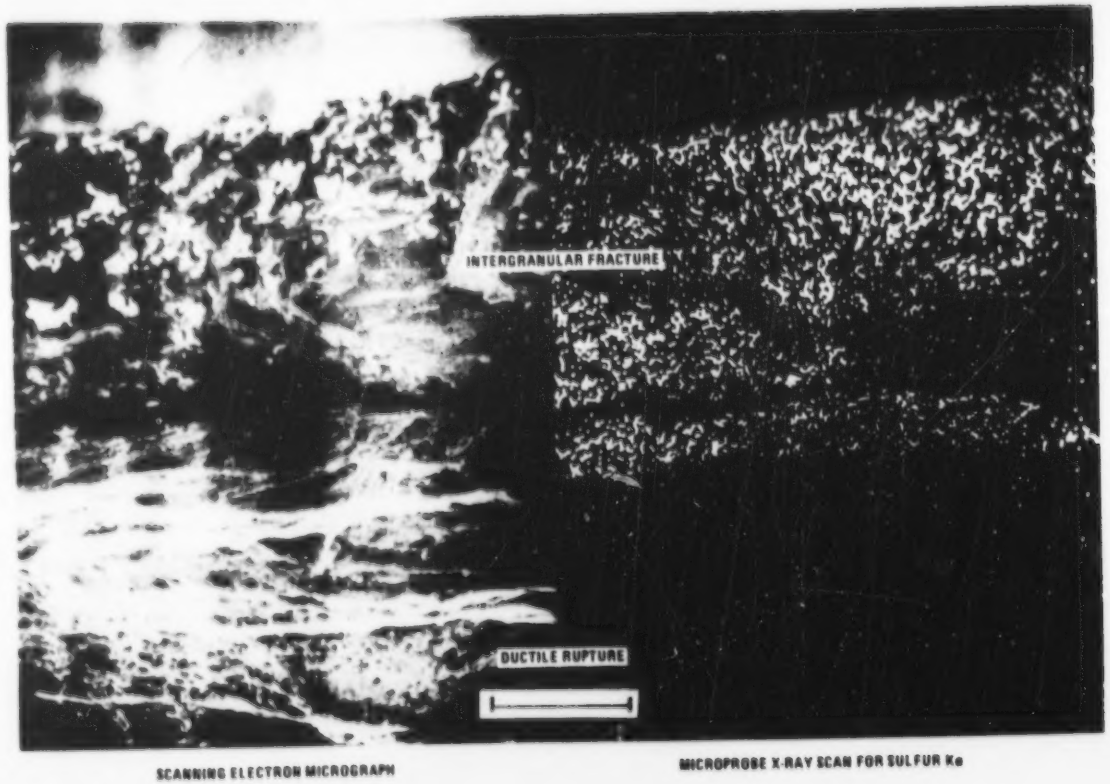

Figure 9. Fracture face cross section of aluminum alloy specimen ruptured by bending after intergranular cracks developed during 1000 hours exposure to air containing SO_2. (Mark = 100 μm)

Table 24. BENDING STRENGTH OF ALUMINUM ALLOY STRESS CORROSION SPECIMENS AFTER EXPOSURE TO DESIGNATED CONTROLLED POLLUTED AIR ENVIRONMENTAL CONDITIONS FOR 1000 HOURS

Stress, KN/m^2	Bending strength and standard deviation, N				Exposure condition	
	High relative humidity		Low relative humidity			
	High SO_2	Low SO_2	High SO_2	Low SO_2		
276	522 ± 107	524 ± 173	503 ± 249	780 ± 185	High O_3	High NO_2
207	693 ± 137	725 ± 31	690 ± 148	760 ± 77		
276	288 ± 175	740 ± 72	570 ± 118	777 ± 14	Low O_3	
207	482 ± 32	764 ± 69	611 ± 115	705 ± 20		
276	632 ± 66	804 ± 58	396 ± 189	657 ± 58	High O_3	Low NO_2
207	512 ± 105	791 ± 30	529 ± 34	685 ± 73		
276	534 ± 32	486 ± 127	591 ± 35	681 ± 176	Low O_3	
207	690 ± 6	712 ± 71	669 ± 123	728 ± 66		

Note: Bending strength values based on three data sets per exposure condition.

Bias may have been introduced into this experiment because of the method used to expose the C-ring specimens. From the standpoint of experimental design, a better method would have been to expose individual specimens randomly placed on a chamber rack, rather than to expose three equally stressed specimens as a group and randomly place the group on the chamber rack. Thus, because of grouping, a possible position effect could be confounded with some tested effects. In analyzing variance, the possibility of arriving at erroneous conclusions of statistical significance for some variables was minimized by assuming that all triple and higher interaction effects were caused by error and using the values of those effects to calculate the error mean square. The resulting F test for significance, therefore, was much more stringent than would have occurred by assuming that the only error was associated to within-sample-variance.

Using this test, only changing the level of SO_2 caused a significant effect on the bending strength at the 99 percent confidence level. Mean bending strengths and standard deviations on the means were 565 N ± 23 N and 713 N ± 18 N for SO_2 levels of 1310 $\mu g/m^3$ and 79 $\mu g/m^3$, respectively. Level of SO_2 accounted for 26 percent of the total variability.

Although stress was necessary to produce cracks, the two levels of stress used in this experiment did not produce significant differences in bending strength.

The results of the clean air exposures are given in Table 25. Assuming that the triple interaction was caused by error, analysis of variance indicated

Table 25. BENDING STRENGTH OF ALUMINUM ALLOY STRESS CORROSION SPECIMENS AFTER EXPOSURE TO DESIGNATED CONTROLLED CLEAN AIR ENVIRONMENTAL CONDITIONS FOR 1000 HOURS

Stress, KN/m^2	Breaking strength and standard deviation, N			
	High relative humidity		Low relative humidity	
	High temp.	Low temp.	High temp.	Low temp.
276	697 ± 187	633 ± 259	700 ± 24	882 ± 61
207	730 ± 79	507 ± 284	822 ± 87	770 ± 101

Note: Bending strength values based on three data sets per exposure condition.

that none of the effects were statistically significant. The mean bending strength and standard deviation on the mean were 717 N ± 36 N.

The mean bending strength of unexposed, unstressed control specimens was 780 N with a standard deviation on the mean of ± 39 N. Thus, stressed specimens exposed in clean air environments experienced an 8.1 percent loss in bending strength. Specimens exposed to 79 $\mu g/m^3$ and 1310 $\mu g/m^3$ of SO_2, respectively, lost approximately 8.6 percent and 27.6 percent of their bending strength.

The lack of complete failures, the relatively large number of cracks perpendicular to the applied stress, and the relatively slow crack growth rates suggest that the effects mechanism is a type of stress-accelerated intergranular corrosion rather than conventional stress corrosion cracking. In a later experiment, specimens exposed stressed for over 2000 hours in clean air at input relative humidity of 80 percent and temperature at 29°C, failed by the conventional stress corrosion cracking mechanism. In each of these specimens, one primary crack with a few secondary cracks developed (Figure 10).

The amount of damage associated with the exposures in polluted air appeared to be proportional to the dose of SO_2. For the amount of time these specimens were exposed at two stress levels, the bending strength appeared to decrease by 1.5 percent for each 100 $\mu g/m^3$ of SO_2.

Longer exposure times may have caused complete failures by a stress corrosion cracking mechanism. Stress-accelerated intergranular corrosion, although a significant problem, is not nearly as critical to parts failures as stress corrosion cracking because the progress of the former can be detected during periodic inspections while the latter cannot.

Longer exposure times at different SO_2 levels are needed to determine if SO_2 significantly promotes stress corrosion cracking.

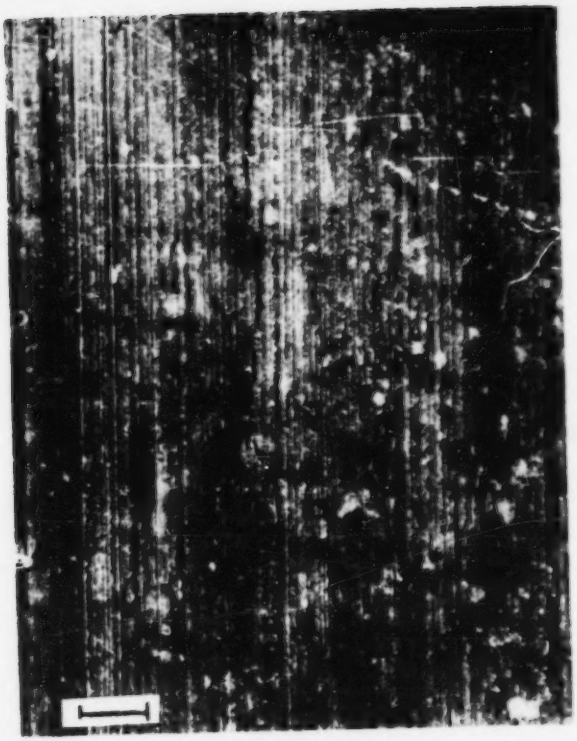

Figure 10. Stress corrosion crack after 2000 hours exposure to clean air. (Mark = 1 mm)

SECTION XI

EFFECTS ON PAINTS

Painted surfaces represent a tremendous area of potential damage by air pollutants. The surfaces, however, are covered by a wide variety of paint formulations that must meet different end use requirements. To evaluate all the various types of paints would be a time consuming and unreasonable task. Therefore, on the basis of discussions with paint industry representatives, four classes of paints, all formulated for exterior exposures, were selected for testing. These were (1) oil base house paint, (2) acrylic latex house paint, (3) vinyl coil coating, and (4) acrylic coil coating. Coil coating, which is applied in factories, is an efficient process for continually dip coating and curing long, flat strips or sheets of metal.

METHODOLOGY

To insure good heat transfer during exposure, 7.6 cm x 12.7 cm aluminum panels served as the substrate for the four types of paint. Vinyl and acrylic coil coating panels were cut from commercially available rolled stock. The two house paints were sprayed on both sides of unprimed panels, which previously had been scrubbed in soapy water, rinsed in distilled water and acetone, and etched with 10% acetic acid. Table 26 shows the nominal paint film thickness on panels for each of the four types of paint. All of the coated panels were conditioned for 48 hours in a constant temperature and relative humidity cabinet at 25°C and 45 percent relative humidity prior to making initial measurements and after each exposure period. This procedure

Table 26. NOMINAL PAINT FILM THICKNESS ON EXPOSED PANELS

Type of paint	Thickness, μm
Oil base house paint*	58
Acrylic latex house paint*	43
Vinyl coil coating	27
Acrylic coil coating	20

*Film allowed to age for three weeks at ambient conditions

allowed each coating to equilibrate, thus minimizing differences in moisture content of the films.

Three panels of each coating were randomly mounted on a chamber exposure rack. After exposure periods of 250, 500, and 1000 hours, the panels were removed from the chambers, cleaned, equilibrated, measured for changes, and, except for final exposure period, returned for additional exposure. The cleaning procedure consisted of wiping off the silicone paste, washing in 5 percent detergent solution followed by a final rinse in distilled water. After measurements were taken, silicone paste was reapplied and the panels were remounted on the rack for the next exposure period.

Two types of measurements were made to assess the amount of damage caused by exposure in the chambers: (1) loss-in-weight and (2) loss-in-film-thickness. Panels were weighed on an analytical balance to within ± 0.1 mg; film thickness was measured to within ± 0.1 μm using a Dermitron thickness tester. Average film thickness on each panel was based on 10 measurements (two measurements at 5 different locations).

Using these measurements, film erosion rates (loss-in-film-thickness per unit of time) were calculated for each of the four paints. Erosion rates are a more appropriate means to assess the effects of pollutants on the useful life of various coatings because paint manufacturers formulate coatings to fail by gradual erosion of the film during exposure. The erosion results for each paint, however, should not be misconstrued as representative of an entire class of paint. Coating formulations may vary considerably within a class of paint. Formulation as well as exposure condition, therefore, will determine erosion characteristics. For example, atmospheric sulfur dioxide will affect paints formulated with calcium carbonate.

RESULTS AND DISCUSSION

The exposure results for the acrylic latex house paint were invalid; this problem will be discussed later. For the remaining paints, however, the various controlled exposure conditions yielded significantly different loss-in-weight values. Furthermore, a definite correlation between loss-in-weight and loss-in-film-thickness was found for each paint. Because units of film thickness rather than weight are more useful in estimating paint life, and because weight measurements were more accurate than film thickness measurements, a conversion factor based on experimental data from initial exposure conditions was calculated for each paint. The conversion factor is the slope of a least squares fit of the loss-in-film-thickness versus loss-in-weight data, which intercepts at the origin. Table 27 gives the resulting factors. Once the conversion factors were determined, film thickness was no longer measured on panels subjected to the remaining exposure conditions. Thus, each loss-in-weight measurement was converted to an equivalent loss-in-film-thickness value prior to data analysis.

Table 27. FACTORS FOR CONVERTING LOSS-IN-WEIGHT TO LOSS-IN-FILM-THICKNESS

Type of paint[a]	Conversion factor, μm/g
Oil base house paint	38.53
Vinyl coil coating	17.94
Acrylic coil coating	34.88

[a]Loss-in-weight data for acrylic latex house paint were invalid.

Previous field exposure studies[15] indicate that paint film erosion rates are normally linear after nine months of exposure; in laboratory studies linearity generally begins after several hundred hours of exposure. Therefore, a linear least squares fit of loss-in-film-thickness values versus exposure time was calculated for each paint for each exposure condition using the following relationship:

$$\mu = A + B\,t \qquad (9)$$

where

μ = loss-in-film-thickness, μm
t = time, yr
A = Constant (intercept)--represents an equivalent thickness of paint film lost during the early stages of aging, μm
B = Constant (slope)--film erosion rate, μm/yr

Thus, if pollutants affect paint films, then different exposure conditions should produce significantly different erosion rates. This hypothesis was examined for each paint.

Oil Base House Paint

Visual examination of these panels revealed that all exposure conditions caused considerable damage to this paint. In some cases the aluminum substrate could be seen through the thinned paint film. Calculated erosion rates were high and confirmed this observation. Table 28 presents the erosion rate values.

Erosion rates ranged from a low of 28.3 to a high 79.1 μm/yr; the average was 60.0 μm/yr. Best estimate of the standard deviation on individual rates was ± 7.1 μm/yr.

Table 29 gives the results of exposure to clean air at the two controlled relative humidities. Eroison rates ranged from 4.2 to 48.6 μm/yr and averaged

Table 28. EROSION RATES OF OIL BASE HOUSE PAINT EXPOSED TO DESIGNATED CONTROLLED POLLUTED AIR ENVIRONMENTAL CONDITIONS

Erosion rate and standard deviation, μm/yr				Exposure condition	
High relative humidity		Low relative humidity			
High SO_2	Low SO_2	High SO_2	Low SO_2		
65.4 ± 7.0	43.7 ± 3.7	45.8 ± 1.9	29.4 ± 2.2	High O_3	High NO_2
79.1 ± 5.4	30.7* ± 7.8	52.6 ± 3.8	28.3 ± 3.3	Low O_3	
72.8 ± 7.2	72.7 ± 12.7	52.4 ± 3.9	48.4 ± 5.8	High O_3	Low NO_2
61.4 ± 3.4	52.1 ± 8.2	60.6 ± 2.8	36.7 ± 8.0	Low O_3	

Note: Erosion rates based on nine data sets per exposure condition except where noted; *six data sets

Table 29. EROSION RATES OF OIL BASE HOUSE PAINT EXPOSED TO DESIGNATED CONTROLLED CLEAN AIR ENVIRONMENTAL CONDITIONS

Erosion rate and standard deviation, μm/yr		Exposure condition
High relative humidity	Low relative humidity	
48.6 ± 9.5	12.5 ± 0.6	High temperature
4.2 ± 2.7	7.5 ± 1.5	Low temperature

Note: Erosion rates based on nine data sets per exposure condition

18.2 μm/yr. Best estimate of the standard deviation on individual rates was ± 5.0 μm/yr. Both average erosion rates and standard deviations were lower when exposed in clean air than in polluted air.

Analysis of variance of the erosion rates are given in Table 30. With little risk, one may conclude that SO_2 concentrations and relative humidity significantly affected the rates of erosion of oil base house paint. The presence of NO_2 apparently increased the weight of the paint film; the amount decreased as the SO_2 level increased. These two effects (direct NO_2 effect and SO_2 x NO_2 interaction effect) were not as significant as the SO_2 and relative humidity effects. These four effects accounted for nearly 81 percent of the between-chamber variability; relative humidity and sulfur dioxide alone accounted for 61 percent.

Table 30. ANALYSIS OF VARIANCE OF OIL BASE HOUSE PAINT EROSION RATES FOR POLLUTED AIR EXPOSURE CONDITIONS

Factor	Contrast	Sum of squares	Degrees of freedom	Mean squares	F	R^2
SO_2	9.272	1375.483	1	1375.483	28.58*	0.35
RH	7.768	965.500	1	965.600	20.06**	0.252
O_3	1.857	55.168	1	55.168	1.15	0.014
NO_2	-5.097	415.650	1	415.650	8.64*	0.109
SO_2 x RH	0.661	6.983	1	6.983	0.15	0.002
SO_2 x O_3	-4.018	258.325	1	258.325	5.37	0.067
SO_2 x NO_2	4.556	332.060	1	332.060	6.90*	0.087
RH x O_3	2.061	67.939	1	67.939	1.41	0.018
RH x NO_2	0.079	0.101	1	0.101	0.00	0.000
O_3 x NO_2	-2.644	111.884	1	111.884	2.32	0.029
Residual		240.666	5	48.133		0.062
Total		3830.059	15			

Notes: F uses the residual mean square in the denominator

R^2 is the coefficient of determination excluding the within chamber variability.

** 99 percent probability level of significance

* 95 percent probability level of significance

A multiple linear regression on SO_2 concentration and relative humidity yielded the following relationship:

$$E = 14.3 + 0.0151 \ SO_2 + 0.388 \ RH. \quad (10)$$

where E = erosion rate, μm/yr
SO_2 = concentration of SO_2, $\mu g/m^3$
RH = relative humidity, %

The 95 percent confidence limits on the calculated erosion rates were ± 23.1 μm/yr. This empirical function predicts that under clean air conditions at 90 percent and 50 percent relative humidity, oil base house paint erosion rates should be 49.2 and 33.7 μm/yr, respectively, within the confidence limits of ± 23.1 μm/yr, 95 percent of the time.

Results of the clean air exposures were consistent with this prediction. A multiple linear regression of the clean air exposure data produced:

$$E = 37.2 + 0.405 \ RH + 1.133 \ T \quad (11)$$

where E = erosion rate, μm/yr
RH = relative humidity, %
T = temperature, °C

The coefficient for the relative humidity effect agrees closely with the similar value in the polluted air function. The clean air function predicts that at 35°C and 90 percent and 50 percent relative humidities, erosion rates should be 38.9 and 22.7 μm/yr, respectively. Both values are well within confidence limits of the polluted air function.

A simpler regression on the product of relative humidity and temperature, which produced a better fit of the clean air data, yielded a linear relationship:

$$E = 11.8 + 0.0179 \ RH \times T \quad (12)$$

This function accounted for 89 percent of the variability as compared with 70 percent for the multiple linear regression. At 35°C and 90 percent and 50 percent relative humidities, calculated erosion rates were 44.7 and 19.6 μm/yr, respectively. These values are even more consistent with the predicted values from the polluted air exposure conditions. The interaction effect of input relative humidity and temperature is consistent with the fact that both must be set to establish a level of moisture in the air. When the moisture level (absolute humidity) remains constant, the relative humidity must decrease if the temperature increases.

Acrylic Latex House Paint

Blisters appeared on the panels exposed to the high SO_2 levels for the first eight exposure conditions. These blisters were examined under a scanning electron microscope and a light microscope. They were caused by a build up of aluminum corrosion products at pits in the substrate. Microprobe analyses revealed high concentrations of sulfur in the corrosion products. The crystalline structure of the material and its water solubility indicated that the product was aluminum sulfate rather than sulfate contaminated aluminum oxide.

Acrylic latex house paint is primarily formulated for application on non-metallic substrates; however, it can be applied to primed metallic surfaces. A desirable characteristic of this paint is permeability to water vapor; this allows a house to "breathe" when considerable differences exist between inside and outside temperatures and relative humidities. Paints that do not have this characteristic may peel because of a build up of condensed moisture between the substrate and film. For this exposure study unprimed aluminum was selected as the substrate because (1) variations in moisture absorption by wood would mask any changes in weight of the paint film, (2) the thickness tester requires an electrical conducting substrate, (3) aluminum is relatively corrosion resistant when boldly exposed to polluted environments, and (4) aluminum is an excellent thermal conductor (to accelerate the formation of dew).

The severe pitting of the aluminum under the paint film was unexpected. The coating may have served as a semipermeable membrane retaining moisture under the surface and excluding oxygen that would tend to passivate the aluminum.

Because of the attack on the substrate, exposures of the acrylic latex house paint in this study were terminated after the completion of the first eight exposure conditions. Stainless steel will be used with this paint in future experiments. Pitting of the substrate beneath the paint film produced significant weight increases that are not a measure of film erosion rate. Therefore, these data were invalid and are not presented.

Vinyl Coil Coating

Visual appearance of this factory applied paint film indicated no damage. Calculated erosion rates for the polluted exposures (Table 31), however, showed that the film eroded but at rates considerably less than the oil base house paint. Values ranged from a low of 1.43 to a high of 5.34 μm/yr; the average erosion rate was 3.29 μm/yr. Best estimate of the standard deviation on individual erosion rates was ± 0.49 μm/yr.

Calculated erosion rates for the clean air exposures are given in Table 32. Erosion rates ranged from 0.114 to 2.49 μm/yr and averaged 1.29 μm/yr.

Table 31. EROSION RATES OF VINYL COIL COATING EXPOSED TO DESIGNATED CONTROLLED POLLUTED AIR ENVIRONMENTAL CONDITIONS

Erosion rate and standard deviation, μm/yr				Exposure condition	
High relative humidity		Low relative humidity			
High SO_2	Low SO_2	High SO_2	Low SO_2		
4.76 ± 0.44	4.67 ± 0.46	1.85 ± 0.41	2.12 ± 0.34	High O_3	High NO_2
4.52 ± 0.62	1.43 ± 0.57	2.33 ± 0.25	2.11 ± 0.24	Low O_3	
5.34 ± 0.44	2.43 ± 0.22	3.15 ± 0.25	3.67 ± 0.68	High O_3	Low NO_2
4.25 ± 0.71	1.43 ± 0.36	4.53 ± 0.42	4.02 ± 0.70	Low O_3	

Note: Erosion rates based on nine data sets per exposure condition.

Table 32. EROSION RATES OF VINYL COIL COATING EXPOSED TO DESIGNATED CONTROLLED CLEAN AIR ENVIRONMENTAL CONDITIONS

Erosion rate and standard deviation, μm/yr		Exposure condition
High relative humidity	Low relative humidity	
2.01 ± 0.27	2.49 ± 0.45	High temperature
0.114 ± 0.088	0.558 ± 0.218	Low temperature

Note: Erosion rates based on nine date sets per exposure condition.

Best estimate of the standard deviation on individual erosion rates was ± 0.287 μm/yr. On the basis of the calculated average erosion rate, vinyl coil coatings would have a life expectency of 20 years in clean air environments.

Results of the analysis of variance are given in Table 33. Four factors appeared to increase the erosion rate of the vinyl coil coating: (1) SO_2 concentrations, and relative humidity interacting individually with concentrations of (2) SO_2, (3) O_3, and (4) NO_2. These four factors accounted for 70.6 percent of the non-error (within chamber) variability.

Simple linear regression on the product of relative humidity and SO_2 concentration yielded

$$E = 2.51 + 1.60 \times 10^{-5} \times RH \times SO_2 \qquad (13)$$

where E = erosion rate, μm/yr
RH = relative humidity, %
SO_2 = concentration of SO_2, $\mu g/m^3$

Table 33. ANALYSIS OF VARIANCE OF VINYL COIL COATING EROSION RATES FOR POLLUTED EXPOSURE CONDITIONS

Factor	Contrast	Sum of squares	Degrees of freedom	Mean squares	F	R^2
SO_2	0.5543	4.916	1	4.916	14.09*	0.186
RH	0.3159	1.597	1	1.597	4.58	0.061
O_3	0.2103	0.708	1	0.708	2.03	0.027
NO_2	-0.3136	1.573	1	1.573	4.51	0.060
SO_2 x RH	0.5602	5.021	1	5.021	14.39*	0.190
SO_2 x O_3	-0.2762	1.220	1	1.220	3.50	0.046
SO_2 x NO_2	-0.1626	0.423	1	0.423	1.21	0.016
RH x O_3	0.4859	3.778	1	3.778	10.83*	0.143
RH x NO_2	0.5556	4.938	1	4.938	14.15*	0.187
O_3 x NO_2	0.1664	0.443	1	0.443	1.27	0.017
Residual		1.745	5	0.349		0.066
Total		26.362	15			

Notes: F uses the residual mean square in the denominator
R^2 is the coefficient of determination excluding the within chamber visibility
* 99 percent probability level of significance

This empirical function accounted for 34 percent of the variability and RH x SO_2 was the only factor that was statistically significant at the 95 percent probability level. The function indicates that at the primary air quality standard of 80 $\mu g/m^3$ for SO_2, this pollutant only contributes between 2.5 and 4.4 percent to the erosion of vinyl coil coatings. Furthermore, the polluted air intercept (2.51) is consistent with the average erosion rate (2.25) for the clean air exposures conducted at the same input temperature of 35°C. The differences between the two values is not statistically significant.

Acrylic Coil Coating

Like the vinyl coil coating, the acrylic coil coating retained its original appearance during exposures. Calculated erosion rates (Table 34) for the polluted exposure conditions were low and ranged from 0.74 to 1.27 µm/yr. The average erosion rate was only 0.57 µm/yr. Best estimate of the standard deviation on individual erosion rates was ± 0.31 µm/yr. Even under the most severe exposure conditions, this particular film can be expected to last at least 15 years.

Table 34. EROSION RATES OF ACRYLIC COIL COATING EXPOSED TO DESIGNATED POLLUTED AIR ENVIRONMENTAL CONDITIONS

Erosion rate and standard deviation, µm/yr				Exposure condition	
High relative humidity		Low relative humidity			
High SO_2	Low SO_2	High SO_2	Low SO_2		
0.83 ± 0.26	1.27 ± 0.20	0.42 ± 0.13	1.29 ± 0.37	High O_3	High NO_2
0.55 ± 0.32	0.43 ± 0.25	0.66 ± 0.25	-0.11 ± 0.15	Low O_3	
1.25 ± 0.71	1.15 ± 0.15	0.41 ± 0.39	0.26 ± 0.40	High O_3	Low NO_2
0.25 ± 0.08	0.74 ± 0.24	0.52 ± 0.28	0.60 ± 0.14	Low O_3	

Note: Erosion rates based on nine data sets per exposure condition.

Table 35 gives the calculated erosion rates for the clean air exposure conditions. Erosion rates ranged from 0.48 to 0.20 μm/yr and averaged 0.09 μm/yr. Best estimate of the standard deviation on individual erosion rates was ± 0.62 μm/yr. On the basis of the calculated average erosion rate, acrylic coil coatings should have a life expectency of over 200 years when exposed in clean air.

Results of the analysis of variance for the polluted air exposures are given in Table 36. Ozone was the most likely factor to affect erosion rates of acrylic coil coatings. A linear regression of the erosion rate data as a function of O_3 level yielded

$$E = 0.159 + .000714\ O_3 \qquad (14)$$

where E = erosion rate, μm/yr
O_3 = concentration of O_3, $\mu g/m^3$

The 95 percent confidence limits on the data were ± 0.98 μm/yr. Although the effect of ozone was statistically significant, for all practical purposes the effect was negligible.

Analysis of variance of the clean air exposure data indicated that neither relative humidity nor temperature had a significant effect on the erosion rate of acrylic coil coatings. The mean value of 0.09 μm/yr was consistent with an erosion rate of 0.52 μm/yr predicted by the empirical function derived from polluted air exposure date.

Table 35. EROSION RATES OF ACRYLIC COIL COATING EXPOSED TO DESIGNATED CONTROLLED CLEAN AIR ENVIRONMENTAL CONDITIONS

Erosion rate and standard deviation, μm/yr		Exposure condition
High relative humidity	Low relative humidity	
0.13 ± 0.15	0.20 ± 1.20	High temperature
0.08 ± 0.12	-0.05 ± 0.19	Low temperature

Note: Erosion rates based on nine data sets per exposure condition.

Table 36. ANALYSIS OF VARIANCE OF ACRYLIC COIL COATING EROSION RATES FOR POLLUTED EXPOSURE CONDITIONS

Factor	Contrast	Sum of squares	Degrees of freedom	Mean squares	F	R^2
SO_2	0.0456	0.0332	1	0.0332	0.13	0.008
RH	0.0587	0.0551	1	0.0551	0.22	0.013
O_3	0.2941	1.3836	1	1.3836	5.50	0.321
NO_2	0.1028	0.1691	1	0.1691	0.67	0.039
SO_2 x RH	0.499	0.0399	1	0.0399	0.16	0.009
SO_2 x O_3	-0.1784	0.5094	1	0.5094	2.02	0.118
SO_2 x NO_2	-0.0989	0.1566	1	0.1566	0.62	0.036
RH x O_3	0.2049	0.6720	1	0.6720	2.67	0.156
RH x NO_2	0.0424	0.0288	1	0.0288	0.11	0.007
O_3 x NO_2	-0.0106	0.0018	1	0.0018	0.01	0.000
Residual		1.2582	51	0.2516		0.292
Total		4.3077	15			

Notes: F uses the residual mean square in the denominator

R^2 is the coefficient of determination excluding the within chamber variabilit

SECTION XII

EFFECTS ON DYED FABRICS

Drapery fabrics were selected for exposure because they represent textiles that are both economically important and subject to fading. Furthermore, they are designed to have fairly long life; however, their useful life may be limited by accumulated fading. Draperies are normally exposed indoors to daily cycles of sunlight and to pollution levels that are generally lower than those existing outdoors.

METHODOLOGY

A large producer of standard-size draperies, which are distributed and sold nationwide, supplied the study with samples of three fabrics (Table 37). The fabrics were popular colors and represented moderate to high volume usage.

Table 37. DESCRIPTION OF DRAPERY FABRICS

Fabric	Color
66% Rayon, 34% Acetate	Royal Blue
66% Rayon, 34% Acetate	Red
100% Cotton duck	Plum

The identity of the dyes on each fabric was unknown. A superficial evaluation, however, revealed that none of the fabrics contained the vulnerable disperse dyes known to fade in the presence of atmospheric nitrogen oxides and/or ozone. The plum colored cotton duck fabric, which faded considerably as later exposure results will show, appeared to be vat dyed.

The drapery fabrics were cut into 8.89 x 6.35 cm panels, mounted in plastic frames, and conditioned for 48 hours at constant temperature (25 ± 0.5°C) and relative humidity (45 ± 1%). The initial color of each fabric panel was then analyzed photoelectrically with a Hunter Model D25A color difference meter. The instrument measures color as a three dimensional point (L,a,b) in space. The (L) value is a measure of lightness, the (a) value of red to green, and the (b) value yellow to blue. Fading is expressed in color difference or fading units (ΔE) and was calculated using the equation:

$$\Delta E = \sqrt{(L_o-L)^2 + (a_o-a)^2 + (b_o-b)^2} \qquad (15)$$

where the subscript "o" refers to initial values.

Beloin describes the color analyzing technique in more detail.[16]

Three replicate panels of each fabric were randomly placed in the exposure chambers in such a way that moisture would not condense on them during the dew cycle. (Moisture is unlikely to condense on household textiles during normal use.) After exposure periods of 250, 500 and 1000 hours, the panels were removed and conditioned at constant temperature and relative humidity, analyzed for color, and, except for the final exposure period, returned to the chambers for additional exposure.

RESULTS AND DISCUSSION

After 1000 hours exposure, the most severe condition--high pollution levels and high relative humidity--caused maximum fading of the drapery fabrics. Color change (ΔE) values for the royal blue, red, and plum colored fabrics were 2.4, 8.7, and 29.1 respectively. A color change less than 3.0 units is difficult to detect by eyesight.

Because most of the fading data appeared to be linearly proportional to exposure time over these relatively short exposure periods, least squares fits of the fading data versus exposure time (through the origin) were calculated. The resulting slopes represent fading rates. Table 38 presents the fading rates for the three drapery fabrics and 16 exposure conditions. Fading rates ranged from a low of 16 fading units per year for the royal blue fabric, to a high of 301 fading units per year for the plum fabric. These values represent initial fading rates and not the amount of fading that would be expected to occur in a year. Under actual long term exposures, fading is a non-linear function of time and fading rates approach zero with time.

The fabrics were also exposed to clean air under different input relative humidity and temperature conditions. These results are given in Table 39; fading rates ranged from a low of 11 to a high of 94 units per year.

Results of an analysis of variance for the three fabrics exposed to the polluted air environments are given in Tables 40, 41, and 42. Using all triple and greater interactions to calculate the residual or error mean square, only relative humidity was a significant factor for both the red and royal blue fabrics. The significant factors for the plum fabric were relative humidity, NO_2, and the interation between relative humidity and NO_2. For all three fabrics, changing (increasing) the input relative humidity produced the greatest effect.

Table 38. INITIAL FADING RATES OF DRAPERY FABRICS EXPOSED TO DESIGNATED CONTROLLED POLLUTED AIR ENVIRONMENTAL CONDITIONS

Drapery fabric color	Initial fading rate and standard deviation, fading units per year				Exposure condition	
	High relative humidity		Low relative humidity			
	High SO_2	Low SO_2	High SO_2	Low SO_2		
Blue	21 ± 10	27 ± 10	18 ± 7	17 ± 3	High O_3	High NO_2
Red	73 ± 9	103 ± 8	60 ± 3	83 ± 12		
Plum	301 ± 89	201 ± 6	120 ± 20	120 ± 4		
Blue	28 ± 15	24 ± 13	70 ± 5	19 ± 1	Low O_3	
Red	80 ± 12	96 ± 11	63 ± 7	81 ± 3		
Plum	261 ± 38	203 ± 7	106 ± 4	122 ± 10		
Blue	26 ± 8	27 ± 11	23 ± 6	16 ± 3	High O_3	Low NO_2
Red	47 ± 7	102 ± 7	66 ± 5	38 ± 6		
Plum	135 ± 19	146 ± 13	90 ± 5	94 ± 5		
Blue	35 ± 14	37 ± 15	17 ± 6	23 ± 8	Low O_3	
Red	98 ± 10	91 ± 5	51 ± 4	33 ± 3		
Plum	142 ± 20	131 ± 13	68 ± 5	80 ± 6*		

Note: Fading rates based on nine data sets per exposure condition except where noted; * 8 data sets.

Table 39. INITIAL FADING RATES OF DRAPERY FABRICS EXPOSED TO DESIGNATED CONTROLLED CLEAN AIR ENVIRONMENTAL CONDITIONS

Drapery fabric color	Initial fading rate and standard deviation, fading units per year			
	High relative humidity		Low relative humidity	
	High temperature	Low temperature	High temperature	Low temperature
Blue	18 ± 10	12 ± 7	15 ± 5	11 ± 4
Red	75 ± 13	16 ± 3	26 ± 2	14 ± 6
Plum	94 ± 12	68 ± 8	48 ± 5	60 ± 7

Note: Fading rate based on nine data sets per exposure condition.

Table 40. ANALYSIS OF VARIANCE OF ROYAL BLUE FABRIC FADING RATES FOR POLLUTED AIR EXPOSURE CONDITIONS

Factor	Contrast	Sum of squares	Degrees of freedom	Mean square	F	R^2
SO_2	-0.0106	0.0018	1	0.0018	0.00	0.000
RH	4.5769	335.1646	1	335.1646	21.31**	0.577
O_3	-1.7506	49.0350	1	49.0350	3.12	0.085
NO_2	-1.8731	56.1376	1	56.1376	3.57	0.097
SO_2 x RH	-0.5094	4.1514	1	4.1514	0.26	0.007
SO_2 x O_3	0.2406	0.9264	1	0.9264	0.06	0.002
SO_2 x NO_2	0.1256	0.4935	1	0.4935	0.003	0.001
RH x O_3	-1.1119	19.7806	1	19.7806	1.26	0.034
RH x NO_2	-1.2019	23.1121	1	23.1121	1.47	0.040
O_3 x NO_2	0.9006	12.9780	1	12.9780	0.83	0.022
Residual		78.6483	5	15.7297		0.136
Total		580.4293	15			

** 99 percent probability level of significance

Table 41. ANALYSIS OF VARIANCE OF RED FABRIC FADING RATES FOR POLLUTED AIR EXPOSURE CONDITIONS

Factor	Contrast	Sum of squares	Degrees of freedom	Mean square	F	R^2
SO_2	-5.505	484.880	1	484.880	1.67	0.063
RH	13.471	2903.593	1	2903.593	9.99*	0.374
O_3	-1.265	25.604	1	25.604	0.09	0.003
NO_2	7.020	788.486	1	788.486	2.71	0.102
SO_2 x RH	-6.320	639.078	1	639.078	2.20	0.082
SO_2 x O_3	-4.456	317.731	1	317.731	1.09	0.041
SO_2 x NO_2	-5.291	447.957	1	447.957	1.54	0.058
RH x O_3	-3.555	202.208	1	202.208	0.70	0.026
RH x NO_2	-5.429	471.324	1	471.324	1.62	0.061
O_3 x NO_2	1.141	20.839	1	20.839	0.07	0.003
Residual		1452.827	5	290.5654		0.187
Total		7754.527	15			

* 95 percent probability level of significance

Table 42. ANALYSIS OF VARIANCE OF PLUM FABRIC FADING RATES FOR POLLUTED AIR EXPOSURE CONDITIONS

Factor	Contrast	Sum of squares	Degrees of freedom	Mean square	F	R^2
SO_2	8.065	1040.708	1	1040.708	2.31	0.016
RH	44.925	32292.091	1	32292.091	71.58**	0.509
O_3	5.768	532.225	1	532.225	1.18	0.008
NO_2	34.193	18706.033	1	18706.033	41.47**	0.295
SO_2 x RH	11.840	2242.970	1	2242.970	4.97	0.035
SO_2 x O_3	2.768	122.545	1	122.545	0.27	0.002
SO_2 x NO_2	9.848	1551.572	1	1551.572	3.43	0.024
RH x O_3	-0.085	0.116	1	0.116	0.00	0.00
RH x NO_2	17.200	4733.440	1	4733.440	10.49*	0.075
O_3 x NO_2	0.373	2.220	1	2.220	0.00	0.000
Residual		2255.571	5	451.114		0.036
Total		63479.491	15			

* 95 percent probability level of significance

* 99 percent probability level of significance

Results of an analysis of variance of the clean air exposure fading data are given in Table 43. When the within-sample-error to calculate values of F was used, the direct effects and the interaction between temperature and relative humidity were all significant at the 99 percent probability level. Using the more stringent test of assuming the triple interaction as the residual error, only the obvious color differences among the fabrics were significant.

The plum fabric, therefore, was the only drapery fabric significantly affected by any of the pollutants; nitrogen dioxide contributed directly and synergistically with relative humidity to increased fading rates. The amount of fading that occurred after 1000 hours of exposure was easily detected visually. Thus, pollutant fading of this drapery fabric could have economic significance if the magnitude of fading under expected ambient conditions is sufficiently large. A dose-response relationship is needed to calculate this magnitude.

The rate of fading at any point in time is expected to be proportional to the concentrations of the reacting ingredients. These ingredients are energy (light and heat), moisture, NO_2, and dye. During the chamber exposures, all ingredient levels except the dye remained constant with time. At infinite time all the dye that is available to react will have reacted to produce maximum fading (ΔE_m). Thus, ΔE_m is a measure of the total amount of dye available to react before fading, and ($\Delta E_m - \Delta E$) is a measure of the amount available at any time (t). For any particular set of conditions:

Table 43. ANALYSIS OF VARIANCE OF FADING RATES FOR CLEAN AIR EXPOSURE CONDITIONS

Factor	Sum of squares	Degrees of freedom	Mean square	F	R^2
RH	987.361	1	987.361	18.11**	0.0665
T	751.292	1	751.292	13.78**	0.0506
Fabric	5966.859	1	2983.430	54.73**	0.4017
RH x T	637.000	1	637.000	11.69**	0.0429
RH x Fabric	399.897	2	199.449	3.67	0.0269
T x Fabric	588.995	2	294.491	5.40*	0.0397
RH x T x Fabric	290.201	2	145.101	2.66	0.0195
Within Sample Error	5233.250	96	54.513		0.3523

** 99 percent probability level of significance
* 95 percent probability level of significance

$$\frac{d\Delta E}{dt} = a_o(\Delta E_m - \Delta E) \tag{16}$$

where $\frac{d\Delta E}{dt}$ = the fading rate.

a_o = a constant that is a function of light, moisture in the air, and NO_2 level.

The amount of fading as a function of time, therefore, is:

$$\Delta E = \Delta E_m (1-e^{-a_o t}) \tag{17}$$

The actual fading data for the plum fabric indicate that the following empirical function is a good approximation:

$$\Delta E = 30[1-e^{-(0.75 + 0.01M + 2.9 \times 10^{-5} \times NO_2 \times M)t}] \tag{18}$$

where ΔE = amount of fading, fading units
M = amount of moisture, mg/m^3, at 25°C and one atmosphere (determined by input relative humidity and temperature)
NO_2 = concentration of NO_2, $\mu g/m^3$
t = exposure time, yr.

Despite the total number of factors that were varied and the simplicity of the approximation, this function accounts for nearly 78 percent of the variability. The degree of fit is shown in Figure 11.

Unacceptable levels of fading are subjective and vary considerably with individuals. Nevertheless, the presence of NO_2 and moisture in the ambient air will synergistically accelerate fading and thus reduce the time required to reach any unacceptable level. This effect can be conveniently expressed in terms of percentage useful life lost. By letting t_1 and t_2 represent the times necessary to reach unacceptable fading in ambient clean air and in ambient air containing NO_2, respectively, then

$$\text{Percentage Life Lost} = \left(\frac{t_1 - t_2}{t_1}\right) 100 \tag{19}$$

Since the level of unacceptable fading is the same for both exposure time periods,

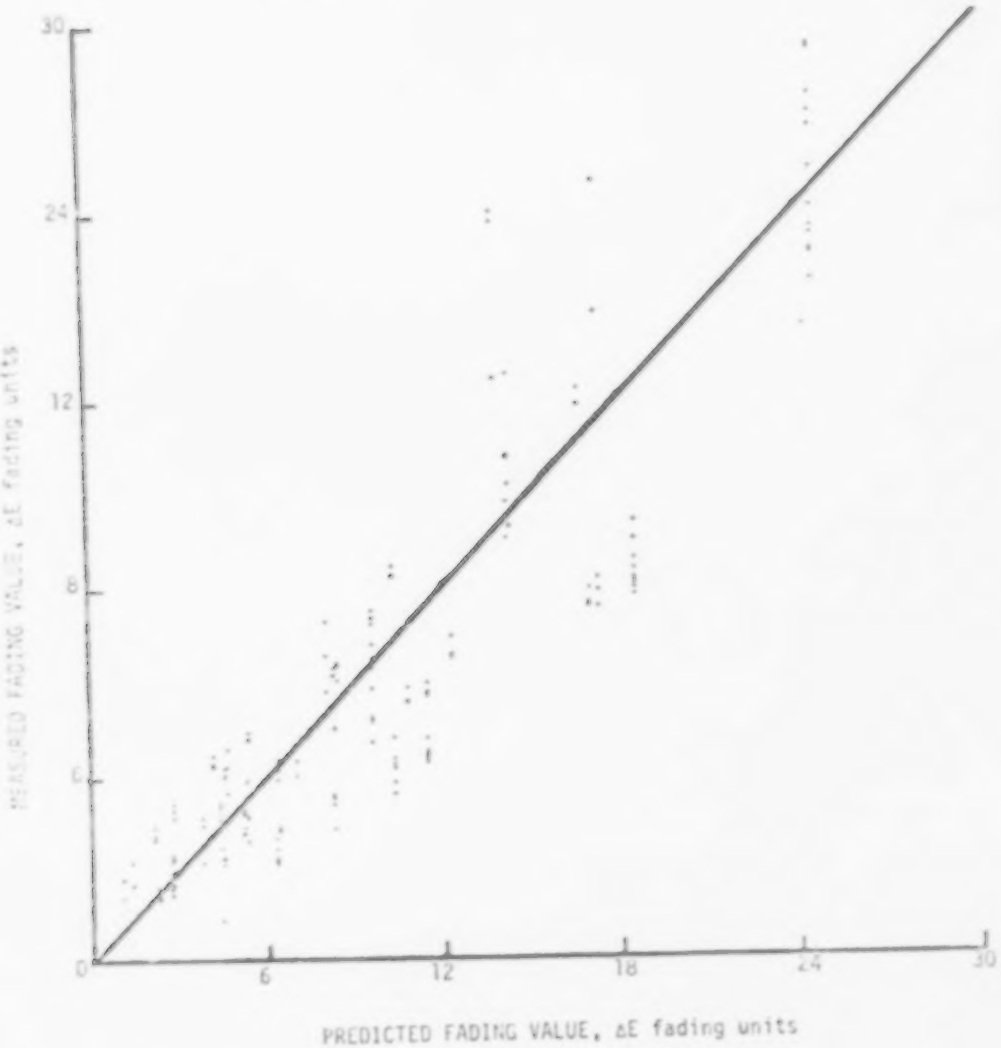

Figure 11. Comparison of predicted and measured fading values for the plum colored fabric exposed to laboratory controlled polluted air and clean air conditions.

$$\Delta E = E_m \left[1-e^{\left(-a_{\circ t_1}\ t_1\right)}\right] = E_m \left[1-e^{\left(-a_{\circ t_2}\ t_2\right)}\right] \quad (20)$$

$$a_{\circ t_1}\ t_1 = a_{\circ t_2}\ t_2 \quad (21)$$

Therefore,

$$\left(\frac{t_1 - t_2}{t_1}\right) 100 = \frac{a_{\circ t_2} - a_{\circ t_1}}{a_{\circ t_2}} \quad (22)$$

Substituting for $a_\circ$ the expression $0.75 + 0.01M + 2.9 \times 10^{-5} \times NO_2 \times M$ and remembering that time t_1 corresponds to exposure in clean air containing no NO_2, the following relationship is derived:

$$\text{Percentage Life Lost} = \frac{2.9 \times 10^{-3} \times NO_2 \times M}{0.75 + 0.01M + 2.9 \times 10^{-5} \times NO_2 \times M} \quad (23)$$

When the plum fabric is exposed to the amount of light used in these exposures, the value 0.75 is a factor associated with fading by light. Since draperies are seldom exposed indoors to such intense light (simulating midday direct sunlight), arbitrarily reducing the factor by 1/2 should provide a more realistic relationship. At 60 percent relative humidity and 25°C, the amount of moisture in the air is approximately 115 mg/m^3. Equation (23), therefore, becomes

$$\text{Percentage Life Lost} = \frac{0.45\ NO_2}{1.93 + 0.0045\ NO_2} \quad (24)$$

Figure 12 is a plot of this function. It predicts that at a concentration of NO_2 equivalent to the national primary ambient air quality standard of 100 $\mu g/m^3$ would reduce the useful life of the plum fabric by 19 percent.

Because only one of three fabrics was appreciably faded by any of the three pollutants, product selection rather than pollution abatement is probably the most economic solution to the fading problem. Before consumers can make this selection, however, textile producers must make them aware of the fading characteristics of fabrics by proper labelling.

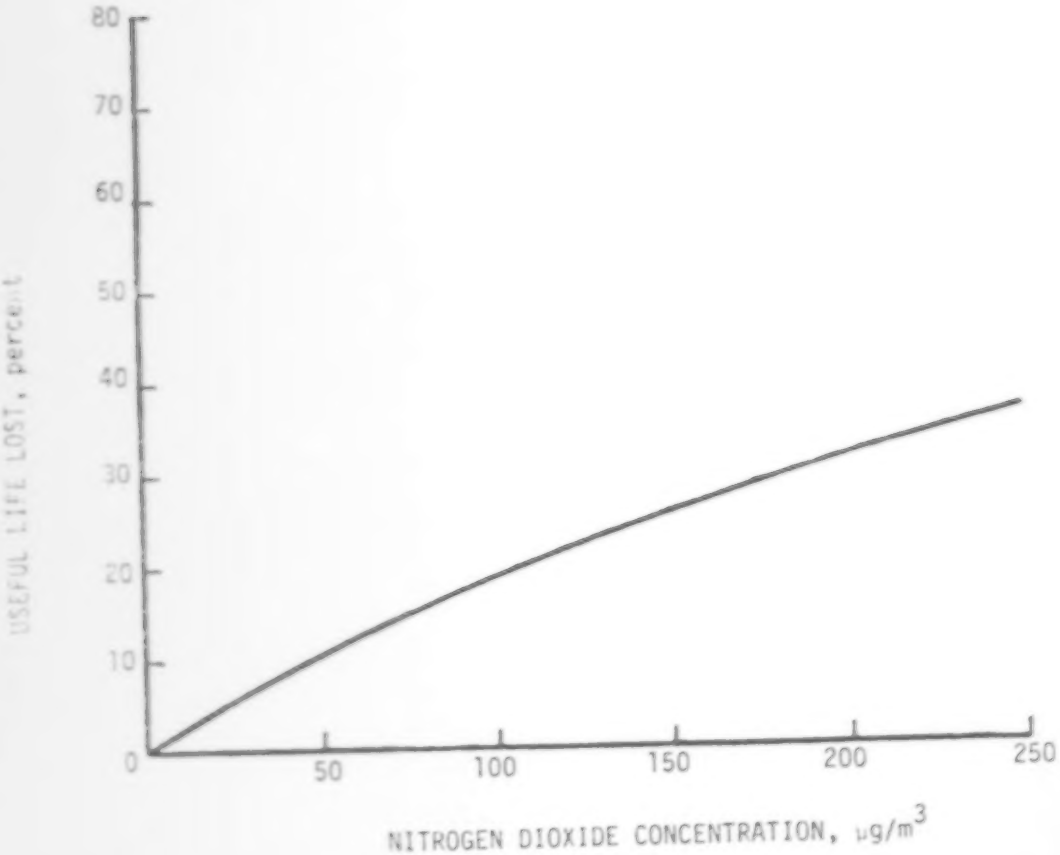

Figure 12. Effect of nitrogen oxide concentration on the fading of the plum colored fabric.

SECTION XIII

EFFECTS ON ELASTOMERS AND PLASTICS

Elastomeric and plastic products are economically important materials that air pollutants could potentially damage and cause a loss in useful life. Two representative and economically significant products were selected for exposure in this study: white sidewall rubber from radial ply tires and extruded white vinyl house siding.

Scientists and engineers have known for many years that atmospheric ozone deteriorates products made from a number of common elastomers. Small cracks that progressively enlarge develop in areas under stress; this effect is called "ozone cracking." The addition of antiozonants to elastomeric formulations offers limited protection against ozone cracking. For rubber tires, this protection is usually sufficient for the useful life of the product.

Because of staining, however, antiozonants are not added to white sidewall rubber. Tire manufacturers normally depend on the use of more resistant elastomers for protection. Over the years this approach has been satisfactory for conventional non-radial tires, but may not hold true for radial tires since tread wear is about twice as long. Therefore, white sidewall failure as a result of ozone cracking could be a limiting factor in the life of radial tires.

Vinyl house siding is a frequently used product because of its long life and essentially maintenance free surface. The presence of air pollutants, however, may cause damage that would reduce the useful life of this product.

METHODOLOGY

Rubber

White sidewall rubber specimens were cut from a top-of-the-line steel belted, rayon cord, radial ply tire. The size of each specimen strip was 1 cm x 9 cm, with the long dimension parallel to the axis of the cord and perpendicular to the white wall strips. The cut edges of the specimens were coated with wax to prevent absorption of moisture and pollutants by the exposed ends of rayon cord.

Special aluminum jigs were used to hold three rubber specimens under a predetermined strain during exposure. For each exposure condition, three specimens were exposed at 10 percent strain and three at 20 percent strain.

The jigs were randomly mounted in the chambers so that dew did not condense on the rubber specimens. Nevertheless, the specimens were exposed to changes in temperature and relative humidity caused by the dew/light cycle.

After each nominal exposure period of 250, 500, and 1000 hours, photomacrographs (10x) were made of the specimens while still under stress. On completion of the 1000-hour exposures, dumbbell tensile specimens were die cut from the exposed strips. Tensile tests were then carried out using an Instron tensile testing machine to determine the breaking strength of the rayon cord.

Vinyl Siding

Specimens measuring 5 cm square were cut from white vinyl house siding and randomly exposed in triplicate. Because appearance is a primary factor limiting the useful life of this product, a change in reflectance was used to assess potential surface effects. Reflectance was measured with a photovolt meter using blue, green and amber filters. For each of the 16 exposure conditions, measurements were taken initially and after each nominal exposure period of 250, 500, and 1000 hours. Specimen surfaces were also examined visually for possible effects.

RESULTS AND DISCUSSION

Rubber

As a result of die cutting the exposed rubber strips into dumbbell tensile specimens, the number of uncut rayon cords per specimen varied from 9 to 12, thus affecting the breaking strength of the specimens. To reflect this variation, tensile test responses were divided by the number of rayon cords and reported as kilograms per cord.

Table 44 presents the tensile test results for the first eight exposure conditions, which included low and high levels of SO_2, O_3 and relative humidity, and low levels of NO_2. Theoretically, pollutants should have no effect on the cord unless ozone cracking penetrates to cord depth. Therefore, an analysis of variance was made on these results as a group. If the analysis showed that the factors --strain, SO_2, O_3 and relative humidity--did not significantly reduce the strength of the cord, tensile tests on specimen exposed to the remaining conditions (high levels of NO_2) could be omitted.

Although the results in Table 44 are incomplete because it includes data from only seven of the eight exposure conditions, an analysis of variance can be made for all but two possible interaction effects. To avoid experimental

Table 44. CORD BREAKING STRENGTH OF WHITE SIDEWALL RUBBER TIRE SPECIMENS EXPOSED UNDER STRESS TO DESIGNATED CONTROLLED POLLUTED AIR ENVIRONMENTAL CONDITIONS FOR 1000 HOURS

Strain	Cord breaking strength and standard deviation, kg/cord				Exposure condition
	High relative humidity		Low relative humidity		
	High SO_2	Low SO_2	High SO_2	Low SO_2	
20%	8.3±0.8	8.1±0.8	9.6±0.8	8.2±0.8	High O_3
10%	8.3±0.3	8.0±0.6	9.5±0.3	8.9±0.3	
20%	8.2±0.7	9.2±0.8	9.2±1.8	Invalid data	Low O_3
10%	11.1±2.1	8.6±0.2	8.3±0.6	Invalid data	

Notes: 1. Cord breaking strength values based on three data sets per exposure condition.

2. Low NO_2 levels were constant for all eight exposure conditions.

bias, however, error mean square was calculated using interaction-effects-variance rather than within-sample-variance. The reasons for this were (1) the three specimens exposed per chamber were grouped together in a single aluminum jig and thus individual specimens could not be placed randomly, and (2) each exposure condition was not replicated. Table 45 gives the analyses of variance for the direct effects.

Table 45. ANALYSIS OF VARIANCE OF TIRE CORD BREAKING STRENGTH FOR STATISTICALLY SIGNIFICANT FACTORS

Factor	Sum of squares	Degrees of freedom	Mean square	F
Relative humidity	0.2408	1	0.2408	0.314
SO_2	1.3333	1	1.3333	1.740
Stress	0.2579	1	0.2579	0.337
O_3	0.6533	1	0.6533	0.852
Error	6.8982	9	0.7664	

None of these factors caused a statistically significant decrease in cord breaking strength, most likely because the pollutants never made contact with the cord. Microscopic examination of the pulled specimens revealed that environmentally induced cracks in the white sidewall rubber did not penetrate to the cord. Thus, rubber specimens exposed to the remaining eight conditions were not subjected to tensile tests.

Figure 13 is a composite macrograph (about 10X) showing the cracking effects that the white sidewall rubber tire specimens developed when exposed under high stress to the 16 polluted air exposure conditions for 1000 hours. Specimens showed a similar but less severe pattern when exposed under low stress.

To assess the degree of rubber cracking, various quantitative methods were considered. The number of cracks intersecting a given length, average crack length within a given area, and summation of crack lengths within a given area were rejected as valid measures of reduced product life. Tire failure should occur at the weakest point. Thus, an extreme rather than an average value should be more meaningful.

Maximum crack length for each macrograph of exposed specimen was used as a measure of damage response. A least squares fit through the origin of the crack length as a function of exposure time was calculated to get a cracking rate. Table 46 shows the mean cracking rates for all 16 exposure conditions and two strain levels. Values ranged from a low of 0 to a high of 3.8 micrometers per hour (μm/hr).

An analysis of variance of these data revealed that only four of 31 possible direct and synergistic effects were statistically significant at the 95 percent confidence level. Included among the insignificant direct and synergistic effects were the two levels of strain; normally, cracking is a direct function of applied strain. Table 47 presents the analysis of variance for the four statistically significant factors.

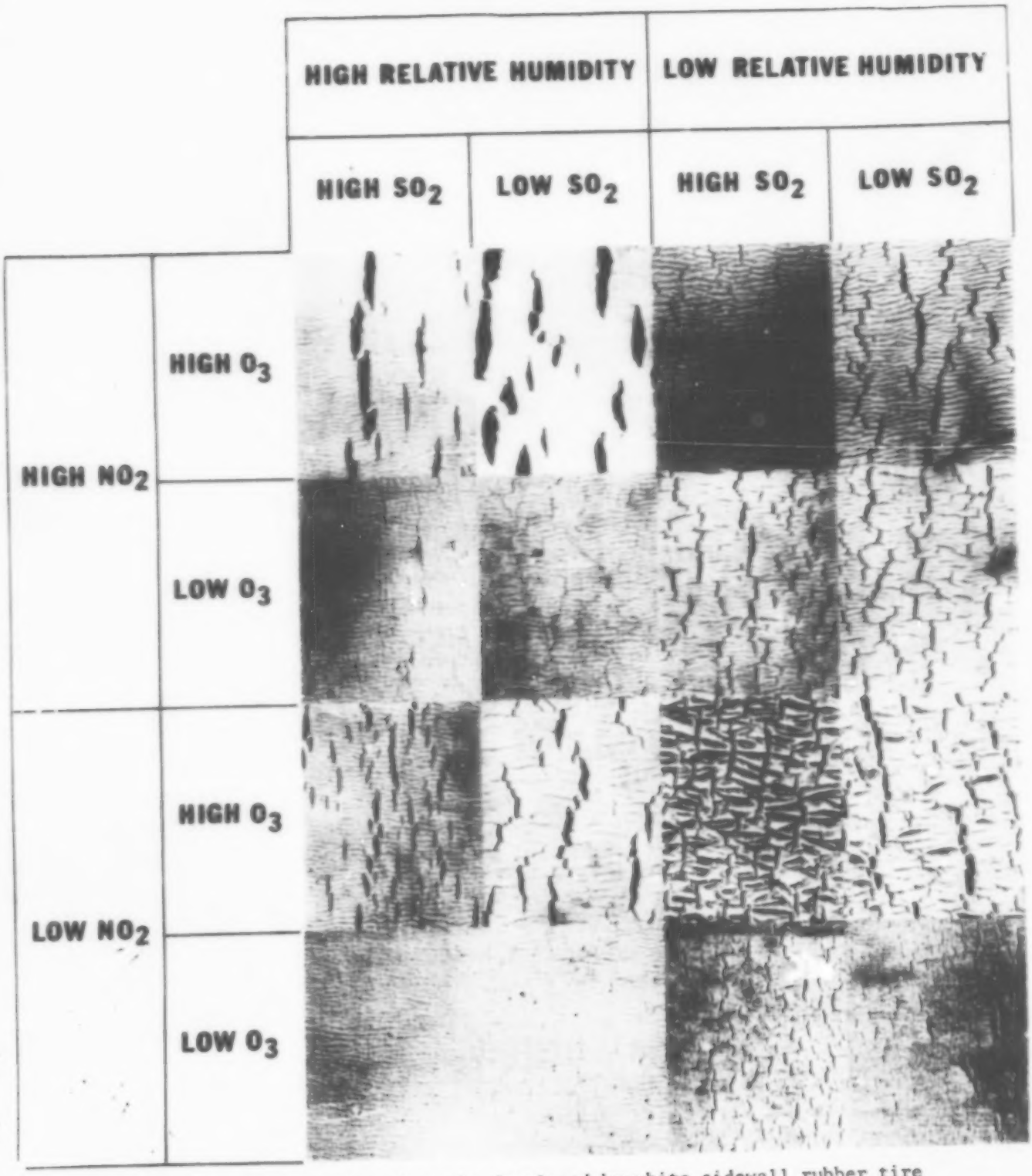

Figure 13. Macrographs of cracks developed by white sidewall rubber tire specimens when exposed under high stress to designated controlled polluted air environmental conditions for 1000 hours.

Table 46. CRACKING RATES OF WHITE SIDEWALL RUBBER TIRE SPECIMENS EXPOSED UNDER STRESS TO DESIGNATED CONTROLLED POLLUTED AIR ENVIRONMENTAL CONDITIONS

Strain	Mean cracking rate and standard deviation, μm/hr				Exposure condition	
	High relative humidity		Low relative humidity			
	High SO_2	Low SO_2	High SO_2	Low SO_2		
10%	1.775 ±1.134	0.761 ±0.638	1.028 ±0.413	2.600** ±0.963	High O_3	High NO_2
20%	2.703 ±0.755	2.361 ±0.460	1.408 ±0.271	3.275* ±1.425	High O_3	High NO_2
10%	0.853 ±0.676	1.377 ±0.477	2.401 ±1.139	2.168* ±2.307	Low O_3	High NO_2
20%	0.993 ±0.325	0.883 ±0.363	1.925 ±0.576	2.466 ±0.576	Low O_3	High NO_2
10%	3.394 ±0.865	3.000* ±0.000	1.756 ±0.721	3.768 ±1.820	High O_3	Low NO_2
20%	2.414 ±0.438	3.760 ±2.909	2.938 ±1.193	3.138 ±0.679	High O_3	Low NO_2
10%	0.0	0.0	1.332 ±0.614	1.331 ±0.753	Low O_3	Low NO_2
20%	0.0	0.684 ±0.408	1.941 ±0.939	1.809 ±0.254	Low O_3	Low NO_2

Note: Cracking rate based on three data sets per exposure condition except where noted; * two data sets; ** one data set.

Table 47. ANALYSIS OF VARIANCE OF RUBBER CRACKING RATES FOR STATISTICALLY SIGNIFICANT FACTORS

Factor	Contrast	Degrees of freedom	Mean square	F
Relative humidity (RH)	-0.32394	1	3.35794	4.45
O_3	0.62269	1	12.40767	16.46*
O_3 x RH	0.33906	1	3.67883	4.88
O_3 x NO_2	-0.44425	1	6.31546	8.38*
Error		1	0.75403	

*99 percent probability level of significance

The rubber specimens did not show a loss in breaking strength because the cracks, which developed during the relatively short exposure periods (1000 hours) used in this study, were not deep enough to expose the cord. As a result air pollutants could not make contact with the cord and cause possible damage. Nevertheless, a loss in strength might have occurred if cracking had been allowed to progress indefinitely.

As would be expected, O_3 concentration was the major factor that accelerated rubber cracking rates. In the absence of O_3, increasing relative humidity appeared to inhibit cracking; however, with O_3 present increasing relative humidity appeared to accelerate cracking. The presence of NO_2 seemed to reduce the damaging effects of O_3.

In the real world, high levels of O_3 and NO_2 generally occur together. Also, the low levels used in this study represented the one hour national primary ambient air quality standard for oxidant (O_3) and the annual average primary ambient air quality standard for NO_2. The average rubber cracking rate at these NO_2 and O_3 levels was 0.89 μm/hr. Crack geometry was such that the depth was less than one fourth the length. Thus, the depth cracking rate into the sidewall would be less that 0.22 μm/hr or less than 2000 μm/yr.

For this particular tire, the depth of the white rubber was 3175 μm and underneath was 1900 μm of black rubber protecting the cord. A developing crack, therefore, must penetrate a distance of 5075 μm before exposing the tire cord. Since black rubber contains antiozonants, the rate of cracking may be less than for the white rubber. However, assuming the rate of cracking for the black rubber to be the same as for the white rubber, it would take about 2 1/2 years for cracks to penetrate to cord depth when continuously exposed to air containing O_3 and NO_2 at levels equivalent to national primary ambient air quality standards. Additional time would be necessary for pollutants to attack the cord.

The calculated crack penetration rate for the white sidewall rubber was based on data derived from continuous exposures at primary ambient air quality standard levels for ozone. But, since average annual O_3 levels in actual real world exposures are much lower, sidewall cracking for this particular tire appears to be an unlikely cause of reduced tire life. Tire tread should wear out first.

Other proprietary tires may be lower quality and produced with white sidewall rubber that is less resistant to ozone. In this case sidewall cracking could pose a problem. Lower quality tires, however, imply less tread wear life. Consequently, tread wear, rather than sidewall failure, should also determine the life of lower quality tires. Thus, the radial tire evaluated in this study should be reasonably representative of all tires with respect to air pollution effects.

Vinyl Siding

Reflectance measurements on vinyl siding specimens essentially did not change during any of the exposure conditions and thus revealed no detectable damage response. Examination with a light microscope and a scanning electron microscope of selected specimens exposed to the most severe environmental conditions also failed to detect any surface damage.

This particular white vinyl house siding was, therefore, highly resistant to damage by gaseous air pollutants as well as moisture and simulated sunlight. Thus, other than soiling by airborne particles, common gaseous air pollutants at ambient concentrations should have no effect on this product.

SECTION XIV

EFFECTS ON MARBLE AND CEMENT

Marble and cement are widely used building materials. Marble is a natural stone and one of the oldest structural as well as artistic materials used by man. Cement is a universal manmade material used as a bonding agent for other materials.

Down through the ages marble has shown a high degree of durability to natural environments. Increasing world wide industrialization and use of fossil fuels, however, have created air pollution. Pollutants not only obscure the asethetic beauty of marble structures with soot and dirt, but also accelerate surface erosion. Furthermore, researchers have found that sulfur dioxide environments promote the formation of water soluble salts which are easily leached away by rain.[17,18]

Evidence that air pollutants attack cement has not been documented but is suspected, mainly because cement contains substances that can react with acid forming pollutants.

METHODOLOGY

Marble

White Cherokee marble with a hone finish was selected for exposure. Specimens measured 2.54 x 2.54 x 0.67 cm.

Two techniques were used to evaluate the effects of pollutants: scanning electron microscopy (SEM) with microprobe analysis, and loss-in-weight. SEM analysis was used to assess evidence of possible surface reactions and subsurface reactions resulting from gaseous diffusion of pollutants (mainly SO_2). To determine if diffusion occurred, x-ray microprobe line scans for sulfur (concentration gradients) were made on cross sections of marble specimens. Sulfur concentration gradients should increase with severity of exposure condition.

Loss-in-weight was the difference between specimen weight before and after 1000 hours exposure. Weights were measured using an analytical balance accurate to the nearest 0.1 mg.

Prior to weighing and exposure, specimens were cleaned and conditioned for 48 hours at constant temperature (25°C) and relative humidity (45%). The cleaning procedure consisted of washing in a 5 percent detergent solution followed by rinsing in distilled water.

For each exposure condition, three specimens were randomly placed on a chamber exposure rack. At the conclusion of 1000 hours exposure, the specimens were removed. Two of the specimens were cleaned, conditioned, and weighed; the remaining specimen was examined by SEM techniques.

Cement

Cement specimens were cast from a water slurry of Portland cement in the form of circular wafers about 2.5 cm in diameter and 0.3 cm thick. Loss-in-weight was used to assess effects using the same methodology as described for marble.

RESULTS AND DISCUSSION

Marble

Examination by SEM of marble specimens exposed for 1000 hours to the most severe conditions (high pollutant levels) revealed that a surface reaction was the primary damage mechanism. A photomicrograph (figure 14) of an exposed surface showed crystalline material containing sulfur atoms, which were identified by x-ray microprobe analysis (figure 15). Although qualitatative analysis was not carried out, the crystalline material was probably calcium sulfate.

X-ray microprobe line scans for sulfur on cross sections of marble specimens revealed penetrations to about 50 μm. However, diffusivity coefficients calculated from sulfur concentration gradients suggested that the diffusion mechanism did not significantly damage this particular marble.

Because SEM analysis was not quantitative, loss-in-weight was a better technique for assessing the magnitude of damage caused by the pollutants. It was assumed that water soluble reaction products removed from the surface of exposed specimens during cleaning accounted for the loss-in-weight. Each loss-in-weight value was converted to an equivalent thickness of calcium carbonate and expressed as an erosion rate-loss in thickness units per year (μm/yr). Table 48 presents average erosion rates (based on two data sets per exposure condition) for all 16 exposure conditions.

An analysis of variance was made on the erosion rate data and the results are shown in Table 49. Sulfur dioxide, relative humidity and ozone were significant factors at the 95 percent probability level. These three factors accounted for 65.7 percent of the variability.

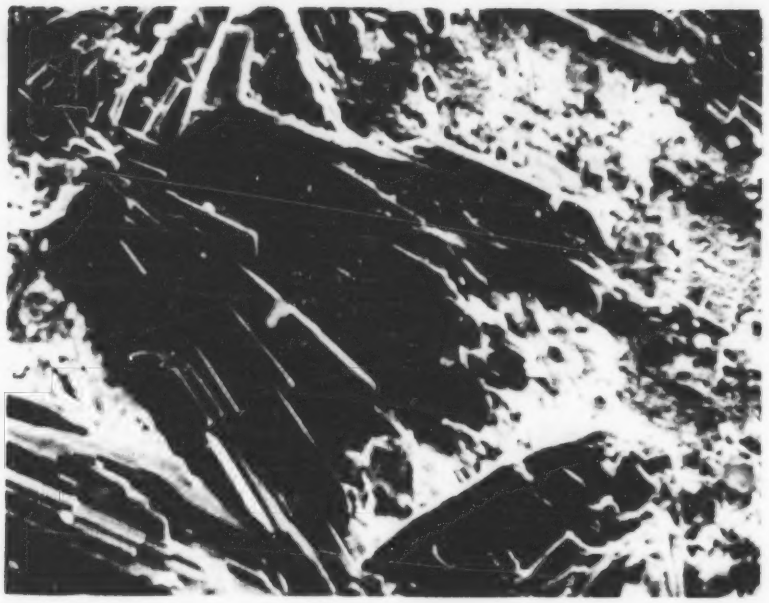

Figure 14. SEM photomicrograph (500X) of marble specimen exposed for 1000 hours to high levels of pollutants and high relative humidity.

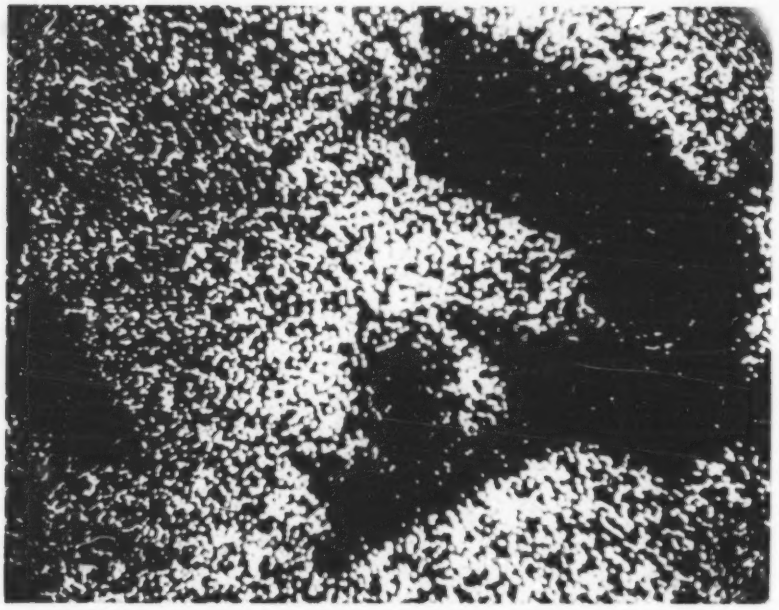

Figure 15. Sulfur x-ray microprobe scan (500X) of marble specimen shown in Figure 14.

Table 48. EROSION RATES OF MARBLE EXPOSED TO DESIGNATED CONTROLLED POLLUTED AIR ENVIRONMENTAL CONDITIONS

Erosion rate and standard deviation, μm/yr				Exposure condition	
High relative humidity		Low relative humidity			
High SO_2	Low SO_2	High SO_2	Low SO_2		
21.8 ± 9.1	7.4 ± 4.9	4.2 ± 9.0	5.0 ± 2.5	High O_3	High NO_2
9.1 ± 10.4	5.7 ± 5.1	1.1 ± 4.6	4.1 ± 3.3	Low O_3	
8.6 ± 10.0	5.6 ± 6.0	7.6 ± 12.9	2.9 ± 2.7	High O_3	Low NO_2
2.9 ± 10.4	3.5 ± 3.4	3.4 ± 2.9	3.8 ± 4.0	Low O_3	

Note: Erosion rate values based on two data sets per exposure condition.

Table 49. ANALYSIS OF VARIANCE OF MARBLE EROSION RATES FOR POLLUTED AIR EXPOSURE CONDITIONS

Factor	Contrast	Sum of squares	Degrees of freedom	Mean square	F	R^2
SO_2	1.814	105.306	1	105.306	15.16*	0.289
RH	1.561	77.969	1	77.969	11.23*	0.214
O_3	1.325	56.154	1	56.154	8.08*	0.154
NO_2	0.526	8.852	1	8.852	1.27	0.024
SO_2 x RH	0.728	16.980	1	16.980	2.44	0.047
SO_2 x O_3	1.066	36.359	1	36.359	5.23	0.100
SO_2 x NO_2	0.143	0.658	1	0.658	0.09	0.002
RH x O_3	0.093	0.276	1	0.276	0.04	0.001
RH x NO_2	0.914	26.736	1	26.736	3.85	0.073
O_3 x NO_2	-0.042	0.057	1	0.057	0.01	0.000
Residual		34.730	5	6.946		0.095
Total		364.077	15			

Notes: F uses the residual mean square in the denominator

R^2 is the coefficient of determination excluding the within chamber variability

* 95 percent probability level of significance

Linear regression of these three factors produced the following relationship:

$$E = -3.31 + 0.078\ RH + 2.95 \times 10^{-3}\ SO_2 + 3.33 \times 10^{-3}\ O_3 \qquad (25)$$

where

E = erosion rate, μm/yr
RH = relative humidity, %
SO_2 = concentration of SO_2, $\mu g/m^3$
O_3 = concentration of O_3, $\mu g/m^3$

Marble specimens exposed to clean air conditions produced data with considerable scatter. An analysis of variance, however, showed no statistically significant effects and mean erosion rates were not significantly different from zero.

Although relative humidity and levels of SO_2 and O_3 appear to accelerate the erosion rate of white Cherokee marble, the exposure results and calculated erosion rates were, nevertheless, quite low. The empirical function predicts that this particular marble will erode only 1 mm in about 300 years when exposed to a somewhat humid (80% RH) environment containing 80 $\mu g/m^3$ (0.03 ppm) SO_2--equivalent to the annual mean national primary ambient air quality standard--and 60 $\mu g/m^3$ (0.03 ppm) O_3. Air pollutants, however, can alter the surface characteristics of marble and therefore reduce inherent asethetic values.

Cement

Accurate weights of conditioned cement specimens were all but impossible to measure under the existing laboratory conditions. The reason for this was that the specimens absorbed atmospheric moisture at an exceedingly high rate. Since a weighing room maintained at constant relative humidity and temperature was not available, effects research on cement was discontinued.

SECTION XV

REFERENCES

1. Clean Air Amendments of 1970. Public Law 91 604. December 31, 1970.

2. Spence, J.W., F.D. Stump, F.H. Haynie, and J.B. Upham. Environmental Exposure System for Studying Air Pollution Damage to Materials. U.S. Environmental Protection Agency, Research Triangle Park, North Carolina 27711. Pub. No. EPA-650/3-75-001. January 1975. 39 p.

3. Spence, J.W. and F.H. Haynie. Design of a Laboratory Experiment to Identify the Effects of Environmental Pollutants on Materials. In: Corrosion in Natural Environments, ASTM STP 558, American Society for Testing and Materials. 1974. p. 279-291.

4. Salmon, R.L. Systems Analysis of the Effects of Air Pollution on Materials. Midwest Research Institute. Contract CPA-22-69-113. January 1970. 187 p.

5. ASTM Standard G 1-67, Recommended Practice for Preparing, Cleaning and Evaluating Corrosion Test Specimens. In: 1970 Annual Book of ASTM Standards, Part 31 Metals--Physical, Mechanical, Nondestructive, and Corrosion Tests, Metallography, Fatigue, Effect of Temperature. 1970. p. 928-931.

6. Guttman, H. and P.J. Sereda. Measurement of Atmospheric Factors Affecting the Corrosion of Metals. In: Metal Corrosion in the Atmosphere, ASTM STP 435, American Society for Testing and Materials. 1968. p. 326-359.

7. Guttman, H. Effects of Atmospheric Factors in the Corrosion of Rolled Zinc. Ibid. p. 223-239.

8. Haynie, F.H. and J.B. Upham. Effects of Atmospheric Pollutants on Corrosion Behavior of Steels. Materials Protection and Performance. 10: 18-21, November 1971.

9. Haynie, F.H. and J.B. Upham. Correlation Between Corrosion Behavior of Steel and Atmospheric Pollution Data. In: Corrosion in Natural Environments, ASTM STP 558, American Society for Testing and Materials. 1974. p. 33-51.

10. Spence, J.W. and F.H. Haynie. Pitting of Galvanized Steel in Controlled Clean Air Environments. To be published by ASTM.

11. Larrabee, C.P. and Ellis, O.B. Report of Subgroup of Subcommittee

VII on Corrosiveness of Various Atmospheric Test Sites as Measured by Specimens of Steel and Zinc. Proc. of American Society for Testing and Materials. 59: 183-201. 1959.

12. Corrosiveness of Various Atmospheric Test Sites as Measured by Specimens of Steel and Zinc. In: Metal Corrosion in the Atmosphere, ASTM STP 435. American Society for Testing and Materials. 1968. p. 360-391.

13. Haynie, F.H. and J.B. Upham. Effects of Atmospheric Sulfur Dioxide on the Corrosion of Zinc. Materials Protection and Performance. 9: 35-40, August 1970.

14. Stress Corrosion Testing Methods. In: Stress Corrosion Testing, ASTM STP 425, American Society for Testing and Materials. 1967. p. 3-20.

15. Campbell, G.G., G.G. Schurr, D.E. Slaevikowski, and J.W. Spence. Assessing Air Pollution Damage to Coatings. Jour. of Paint Technology. 46 (593): 59-71, June 1974.

16. Beloin, N.J. Fading of Dyed Fabrics Exposed to Air Pollutants: A Chamber Study. Textile Chemist & Colorist. 5: 128-133, July 1973.

17. Turner, T.H. Damage to Structures by Atmospheric Pollution. Smokeless Air (Oxford, Eng.). 23: 22-26, April 1952.

18. Braun, R.C. and M.J.C. Wilson. The Removal of Atmospheric Sulphur by Building Stones. Atmospheric Environment (London). 4(4): 371-378, 1970.